TRIBOLOGY TRANSACTIONS
2018, VOL. 61, NO. 2, 304–324
https://doi.org/10.1080/10402004.2017.1319524

stle
Society of Tribologists and Lubrication Engineers

Check for updates

New Stress-Based Fatigue Life Models for Ball and Roller Bearings

Pradeep K. Gupta[a] and Erwin V. Zaretsky[b]

[a]PKG Inc., Clifton Park, NY, USA; [b]Erwin V. Zaretsky, PE, Consulting Engineer, Chagrin Falls, OH, USA

ABSTRACT

New stress-based life models are introduced to define "dynamic stress capacity" in rolling bearings for the first time. The generalized stress capacity equations are formulated, for both point and line contacts, in terms of distinct geometrical and materials parameters while the empirical constants are now material independent. Life equations are first developed for individual rolling element to race contacts and then statistically combined to estimate lives of both races, rolling elements, and, finally, the whole bearings for both ball and roller bearings. An estimate of the empirical constant for the ball bearing equation is derived by regression analysis of available experimental data. The applicable constant for roller bearings is then derived by relating the ball and roller bearing constants to the fundamental subsurface fatigue hypothesis applicable to both point and line contacts. For AISI 52100 bearing steel at room temperature, life predictions with the new stress-based equations are in complete agreement with those currently provided by widely used load-based formulations, where the empirical constant contains the elastic properties of AISI 52100 bearing steel. In addition to these life equations based on the magnitude and depth of maximum orthogonal subsurface shear stress and the volume of material stressed, a new model that eliminates life dependence on the depth of maximum orthogonal shear stress and relates life to only the subsurface maximum shear stress and the stressed volume is presented. Though the predicted life estimates with the currently used and newly introduced life models are comparable in the contact stress range of 2 to 3 GPa, the new model provides significantly higher lives at low contact stresses.

ARTICLE HISTORY
Received 29 October 2016
Accepted 10 April 2017

KEYWORDS
Rolling element bearing; rolling element bearing fatigue; dynamic load capacity; dynamic stress capacity; rolling bearing life prediction; ADORE

Introduction

Harris *(1)* states,

> Tallian *(2)* defined three eras of modern rolling bearing development: an '*empirical*' era continuing through the 1920s; a '*classical*' period lasting through the early 1950s; and the '*modern*' era. Through the *empirical, classical* and well into the *modern* era, it was said that even if rolling bearings are properly lubricated, properly mounted, protected from dirt and moisture, and otherwise properly operated, they will eventually fail because of (rolling-element) fatigue of surfaces in rolling contact.

The first analytical development for rolling element bearing life prediction may be credited to the work of Palmgren (Pamgren *(3)*; Zaretsky *(4)*). Later, based on the statistical techniques developed by Weibull *(5), (6)*, Lundberg and Palmgren *(7), (8)* presented analytical expressions to compute fatigue lives of rolling element bearings. The survival probability was stated to be proportional to the maximum subsurface orthogonal shear stress raised to an empirical exponent; the depth at which this shear stress occurs, raised to another empirical exponent; and the volume of the material stressed. These parameters were related to the classical Hertzian elastic contact solutions between the rolling elements and the bearing races. The contact lives were then statistically summed to derive lives of the races and the complete bearing. Contact life was expressed in terms of a dynamic load capacity, defined as a load under which the contact will survive for one million revolutions of the rotating race with a prescribed survival probability (usually 90%). The associated proportionality constant and the empirical exponents were estimated by correlating the analytical life predictions to experimental lives of bearings made with pre-1940 air-melt AISI 52100 bearing steel. At that time, virtually all rolling element bearings were manufactured with this common bearing steel. Thus, the elastic properties of this material were incorporated as part of the empirical constant. These Lundberg-Palmgren *(7), (8)* life equations, denoted as original LP equations in this article, have been used in virtually all bearing software development and they are still considered as conventional state of the art in rolling bearing life prediction. The LP life equations have also been incorporated with some modification into the American National Standards Institute (ANSI), American Bearing Manufacturers Association (ABMA), and the International Standards Organization (ISO) as standard means for estimating load ratings and life of ball and roller bearings (ANSI/AFBMA 9:1990 (R2000) *(9)*; ANSI/AFBMA 11:1990 (R2008) *(10)*; ISO 281:2007 *(11)*).

Since the 1950s, because fatigue was the primary mode of bearing failure, the advancements in materials and manufacturing technologies have continued to improve bearing fatigue resistance. As a result, the observed bearing fatigue life in 1992 was as much as 200 times the attainable life in 1940 (Zaretsky *(12)*). It is estimated

CONTACT Pradeep K. Gupta guptap@pradeepkguptainc.com; Erwin V. Zaretsky ezaretsky@sbcglobal.net

Color versions of one or more of the figures in the article can be found online at www.tandfonline.com/utrb.

Pradeep K. Gupta is an STLE Life Member.
Erwin V. Zaretsky is an STLE Life Fellow.
Review led by Nick Weinzapfel.

© 2018 Society of Tribologists and Lubrication Engineers

Nomenclature

A = Empirical constant in point contact dynamic stress capacity equation (units depend on values of empirical exponents c, h, and m)
$\hat{A}$ = Empirical constant in point contact dynamic load capacity equation (units depend on values of empirical exponents c, h, and m)
a = Major contact half width (m or in.)
a_1 = Reliability factor
a^* = Dimensionless major contact half width for point contact
B = Empirical constant in line contact dynamic stress capacity equation (units depend on values of empirical exponents c, h, and m)
$\hat{B}$ = Empirical constant in line contact dynamic load capacity equation (units depend on values of empirical exponents c, h, and m)
b = Minor contact half width (m or in.)
b^* = Dimensionless minor contact half width for point contact
c = Shear stress exponent
D = Rolling element diameter (m or in.)
d = Contact track diameter on race (m or in.)
E = Modulus of elasticity (Pa or lbf/in^2)
E' = Effective elastic modulus parameter for contact surfaces (Pa or lbf/in^2)
E'_o = Effective elastic modulus parameter for AISI 52100 bearing steel (Pa or lbf/in^2)
F = Comulative probability function
G = Geometric parameter in point contact dynamic stress capacity equation (units depend on values of empirical exponents c, h, and m)
$\hat{G}$ = Geometric parameter in point contact dynamic load capacity equation (units depend on values of empirical exponents c, h, and m)
$\overline{G}$ = Geometric parameter in line contact dynamic stress capacity equation (units depend on values of empirical exponents c, h, and m)
$\overline{\hat{G}}$ = Geometric parameter in line contact dynamic load capacity equation (units depend on values of empirical exponents c, h, and m)
h = Subsurface shear stress depth exponent
K = Constant in fundamental life equation (units depend on values of empirical exponents c, h, and m)
L = Fatigue life (h)
m = Weibull modulus or slope
N = Life in number of stress cycles
n = Number of rolling elements
p_H = Maximum Hertz contact pressure (Pa or lbf/in^2)
p_{Hc} = Dynamic stress capacity (Pa or lbf/in^2)
Q = Contact load (N or lbf)
Q_c = Dynamic load capacity (N or lbf)
S = Comulative survival probability
u = Number of stress cycles of revolution of rotating race
V = Stressed volume (m^3 or in^3)
V_m = Stress volume above maximum subsurface shear stress (m^3 or in^3)
V_o = Stress volume above maximum orthogonal subsurface shear stress (m^3 or in^3)
w = Effective contact width (m or in.)
z_m = Depth of maximum subsurface shear stress (m or in.)
z_o = Depth of maximum orthogonal subsurface shear stress (m or in.)
ζ = Ratio of subsurface shear stress to minor contact half width
η = Ratio of effective contact width to major contact half width
$\dot{\theta}$ = Rolling element orbital velocity (rpm)
κ = Model constant
λ_E = Material parameter (ratio of E' to E'_o)
υ = Poisson's ratio
ξ = Ratio of subsurface shear stress depth to minor contact half width
ρ = Curvature (1/m or 1/in.)
σ = Any stress (Pa or lbf/in^2)
τ_m = Maximum subsurface shear stress (Pa or lbf/in^2)
τ_o = Maximum orthogonal shear stress (Pa or lbf/in^2)
Φ = Dynamic stress capacity adjustment factor
Ω = Race angular velocity (rpm)
ω_b = Rolling element angular velocity (rpm)

Subscripts

10 = 10% failure probability (90% survival probability)
GZ = Newly introduced GZ model
i = Race (outer = 1, inner = 2)
j = Rolling element index (1 to *n*)
LP = Lundberg-Palmgren model
r = Rotating race
S = Survival probability
s = Stationary race

that today, the bearing life could be as high as 400 times the attainable life in 1940. Though certain "life modification factors," applied on the basic LP life predictions (Zaretsky *(13)*; Tallian *(14)*) have been developed to account for these life improvements, Ioannides and Harris *(15)* have introduced a shear stress limit below which the bearing would have an infinite life. The model, so developed, has also been introduced in the ISO Standard ISO 281:2007 *(11)*. However, the subject of the existence of a shear stress limit for through-hardened bearing steels, such as AISI 52100 steel, remains controversial (Shimizu *(16)*; Zaretsky *(17)*).

Zaretsky *(18), (19)* postulated that becausee rolling element fatigue is a "high-cycle fatigue" process, the life dependence on depth of the cyclic shear stress, as implemented in the LP equations, should be eliminated. In addition, he proposed that, unlike the LP formulation, the stress function should be expressed in terms of maximum shear stress, and any applicable stress exponent should be independent of data variability. Though this work was published in 1987, it was never implemented as a viable life equation until the recent work of Gupta, et al. *(20)*, who made the first attempt to examine the significance of such a life model, while generalizing the LP dynamic load capacity equation to take the material elastic properties out of the empirical constant for better modeling of modern materials.

Following the generalization of the LP dynamic load capacity equation for arbitrary material properties, and after establishing the practical significance of the work carried out by Zaretsky *(18)*, the present work extends the work of Gupta, et al. *(20)*, which was limited to ball bearings, as follows:

1. A new life equation, based on the work by Zaretsky *(18)* is introduced and differences in life prediction with the LP model are further evaluated parametrically for both ball and roller bearings.
2. Similar to the dynamic load capacity introduced by Lundberg and Palmgren *(7), (8)* the present work introduces a "dynamic stress capacity" and formulates generalized life equations in terms of stress rather than load. The objective is to ease future implementation of any limiting shear stress fatigue limit, similar to the one proposed by Ioannides and Harris *(15)*, and to provide a life modeling capability to better investigate the role of residual stresses, which are common in case-hardened materials, and hoop stresses in the races, which result from both high rotational speeds and increasing interference fits.
3. In addition to life equations for the bearing races, the current work presents a life equation of rolling elements. The bearing life is thus segmented into the life of bearing races and rolling elements, where the empirical life constants and associated stress exponents may be varied independently over the races and rolling elements. It is anticipated that such a generalization will provide the needed framework for modeling of modern hybrid bearings where the parameters of ceramic rolling elements may vary widely from those for the steel races. Likewise, the generalized life equations with distinct material parameter permit realistic life modeling with upcoming low-elastic-modulus materials, such as nickel–titanium alloys (60NiTi or Nitinol), as introduced by Dellacorte *(21)*.
4. Because both the fundamental works of Lundberg and Palmgren *(7), (8)* and Zaretsky *(18), (19)* relate life to subsurface stresses, and the implementation for both ball and roller bearings is based on a common hypothesis, the empirical constants in life equations of ball and roller bearings may be related to each other. Thus, the constants in the life equations for roller bearings, presented in the current work, are related to those developed for ball bearings. Distinct equations are presented to show the relationship between ball and roller bearing constants. The objective here is to demonstrate that once the constants are validated against experimental data for ball bearings, the roller bearing constants are also defined to a great extent.
5. The experimental data sets used by Gupta, et al. *(20)* are used to recalibrate the empirical life constants for the new life equations for ball bearings, where the bearing life is segmented into lives of races and balls. These validated constants are then used to derive the applicable constants for roller bearings.
6. For parametric evaluation of the models, although in the current work the newly developed life equations are implemented in the bearing dynamics code ADORE (Gupta *(22)*), the life equations are easily adaptable to any computer code. In fact, a greatly simplified approach to implement the new life equations in absence of the availability of detailed elastic contact solutions is also included in the article.
7. With the objective of easing the transition of relating life to stress rather than load, the equivalent dynamic load capacity equations are also included in one of the appendices to this article.

It is expected that the new life equations will provide an avenue to interface bearing life prediction to thermal interactions in the bearings, where the material properties may be temperature dependent. In addition, discrete modeling of rolling element bearing life may result in improved understanding of the role of ceramic materials in hybrid bearings.

Analytical formulations

Weibull distribution for failure analysis

The early works of Weibull *(5), (6)* generally constitute the foundation of most failure analysis. In most general form, the commonly used Weibull distribution defines the cumulative failure probability, F, as

$$F(N) = 1 - e^{-\left(\frac{N-N_o}{\overline{N}}\right)^m}, \qquad [1]$$

where N is the number of cycles to failure, N_o is a location parameter, $\overline{N}$ is a scaling parameter, and m is shape parameter, commonly known as the Weibull slope or modulus. For fatigue failures, the location parameter is generally set to zero, and the life is commonly expressed in terms of a two-parameter distribution, where the cumulative survival probability, S, is expressed as

$$S = [1 - F(N)] = e^{-\left(\frac{N}{\overline{N}}\right)^m} \text{ or } \ln\frac{1}{S} = \left(\frac{N}{\overline{N}}\right)^m. \qquad [2]$$

Additionally, based on simple experimental observations, Weibull postulated that the survival probability is related to the product of some function of applied stress and the stressed volume

$$\ln\frac{1}{S} \sim \int_V f(\sigma)dV. \qquad [3]$$

Fundamental LP model

Based on a large amount of bearing failure data and the above works of Weibull, Lundberg and Palmgren *(7), (8)* related bearing life to the maximum subsurface orthogonal shear stress, its depth below the surface, and the volume of material stressed. After fitting the experimental bearing failure data to the Weibull distribution, bearing life with 90% survival probability, which is commonly referred to N_{10}, was defined as

$$\left(\frac{1}{N_{10}}\right)^m = K_{LP}\frac{\tau_o^c V_o}{z_o^h}, \qquad [4]$$

where τ_o is the maximum orthogonal subsurface shear stress, z_o is the depth below the surface where this stress occurs, V_o is the applicable stressed volume, and K_{LP}, c, h, and m are empirical

constants derived by fitting the experimental bearing life data to the model. Equations [2] and [4] can now be combined to derive a generalized LP equation to express the life with arbitrary survival probability as

$$\left(\frac{1}{N_S}\right)^m = K_{LP}\frac{\tau_o^c V_o}{z_o^h}\frac{\ln\frac{1}{0.90}}{\ln\frac{1}{S}} = \frac{K_{LP}}{a_1}\frac{\tau_o^c V_o}{z_o^h}, \quad [5]$$

where $a_1 = \frac{\ln\frac{1}{S}}{\ln\frac{1}{0.90}}$ is commonly referred to as a reliability factor. In addition, the number of stress cycles, N_s, may be related to the number of revolutions of the rotating race, L_s (normally measured in terms of millions), and the number of stress cycles per revolution, u,

$$N_s = uL_s. \quad [6]$$

Substitution of Eq. [6] in Eq. [5] yields the fundamental LP life equation:

$$\left(\frac{1}{L_S}\right)^m = \frac{K_{LP}}{a_1}\frac{\tau_o^c V_o}{z_o^h}u^m. \quad [7]$$

The above fundamental equation applies to each individual rolling element–to-race contact in both ball and roller bearings for computing the life of both the races and rolling elements. The maximum orthogonal shear stress, its depth, and the stressed volume may all be related to the Hertzian contact pressure. These relationships are, of course, different for point and line contacts and, when substituted, the life equations for ball and roller bearings may be derived, as will be discussed later.

Cycling frequency

Normally in most applications when one of the races is fixed while the other rotates with a prescribed angular velocity, all lives are measured in terms of revolutions of the rotating race. Therefore, the applicable cycling frequency is defined as the number of stress cycles per revolution of the rotating race. This frequency may be very easily defined when the angular velocities are referenced to a coordinate frame, which travels with the rolling element as it orbits around the bearing. In other words, the number of cyclic contacts on the race per unit time is simply defined by the race angular velocity relative to the rolling element orbital velocity. Likewise, the number of cyclic contacts on the rolling element per unit time is equal to rolling element angular velocity relative to its orbital velocity. Thus, for any rolling element (i, $i = 1$, n, n being the number of rolling elements), if the orbital velocity is $\dot{\theta}_i$ and the angular velocity is ω_i, the cycling frequency, u_{ji}, on the race (j, $j = 1$ for outer and 2 for inner) with an angular velocity Ω_j is defined as

$$u_{ji} = \frac{|\,\Omega_j - \dot{\theta}_i\,|}{\Omega_r}, \quad [8]$$

where Ω_r is the angular velocity of the rotating race. The corresponding cycling frequency on the rolling element, which, of course, will be same for both outer and inner race contacts, is written as

$$u_i = \frac{|\,\omega_i - \dot{\theta}_i\,|}{\Omega_r}. \quad [9]$$

Most commonly used implementations of the LP life model only consider bearing life in terms of lives of the outer and inner races. In addition, it is assumed that all rolling elements move with a constant epicyclic velocity, which is essentially defined by the bearing geometry and the prescribed angular velocity of the rotating race. Thus, the cycling frequency on a pertinent race is expressed by a simple algebraic equation that contains the bearing geometry, number of rolling elements, and angular velocity of the rotating race. In the current more generalized formulation, however, the lives of both the rolling elements and the races that result from each individual contact are first computed and then statistically summed to arrive at the lives of each bearing element and the bearing as a whole. Thus, the generalized expressions, as defined by Eqs. [8] and [9], are used.

New fundamental GZ model

As discussed earlier by Gupta, et al. *(20)*, Zaretsky *(18)* proposed three basic modifications to the LP model: life dependence on depth of subsurface shear stress should be eliminated; the critical failure stress should be the maximum shear stress; and the shear stress life exponent in the life equation should be independent of data variability or Weibull modulus. With these modifications, the resulting life model reverts back to the original postulation by Weibull *(5), (6)*, where the survival probability is stated as proportional to the product of a stress function and the stressed volume. To distinguish this model from the fundamental LP model, this formulation, as presented below, is denoted the "GZ model." Elimination of life dependence on depth of subsurface shear stress is simply accomplished by setting the exponent $h = 0$; the maximum subsurface orthogonal shear stress τ_o is replaced by the maximum subsurface shear stress τ_m; and elimination of data variability in the stress life exponent is simply accomplished by changing the shear stress exponent from c to cm in the LP fundamental equation [7]. Because the depth of maximum shear stress will be different from the depth of maximum orthogonal shear stress, the stressed volume is replaced by V_m. Thus, the new fundamental GZ life equation is written as

$$\left(\frac{1}{L_S}\right)^m = \frac{K_{GZ}}{a_1}\tau_m^{cm}V_m u^m. \quad [10]$$

The empirical constant, K_{GZ}, is again determined by correlation of predicted life with experimental data. Note that the above fundamental equations [7] and [10] for the LP and GZ models, respectively, are applicable for both line and point contacts.

When the classical point and line contact solutions, as documented by Harris and Kotzalas *(23)* and summarized in Appendix A, are substituted in Eqs. [7] and [10], the applicable life equations for the races and rolling elements in both ball and roller bearings may be expressed in terms of the Hertzian contact pressure, p_H. Then, similar to the commonly used dynamic load capacity, which defines a contact load under which the contact can survive one million revolutions of the rotating race, a "dynamic stress capacity" may be defined as the contact pressure

under which the contact survives one million revolutions of the rotating race. The contact lives may then be defined in terms of the dynamic stress capacity. Finally, the applicable life equations for rolling elements, outer and inner races, and the entire bearing may be developed. A summary of these relations is presented below and the algebraic details related to the derivation of the equations are omitted for brevity.

LP race life equations for ball bearings

At each ball-to-race contact, the race life is written as

$$\frac{1}{L_{LP}} = \left(\frac{p_H}{p_{HcLP}}\right)^{\frac{c+2-h}{m}} \quad [11a]$$

Dynamic stress capacity,

$$p_{HcLP} = \Phi_{LP} A_{LP} \kappa_{LP}^{-\frac{1}{c+2-h}} \lambda_E^{\frac{2-h}{c+2-h}} G_{LP}^{-\frac{1}{c+2-h}} u^{-\frac{m}{c+2-h}} \quad [11b]$$

$$\text{Life constant, } A_{LP} = \left[\frac{\pi^{h-3}}{K_{LP} E_o^{'h-2}}\right]^{\frac{1}{c+2-h}} \quad [11c]$$

$$\text{Constant, } \kappa_{LP} = \frac{\eta \zeta_{LP}^c \xi_{LP}^{1-h}}{a_1} \quad [11d]$$

$$\text{Shear stress ratio, } \zeta_{LP} = \frac{\tau_o}{p_H} = 0.25 \text{ (default)} \quad [11e]$$

$$\text{Shear stress depth ratio, } \xi_{LP} = \frac{z_o}{b} = 0.50 \text{ (default)} \quad [11f]$$

$$\text{Contact width ratio, } \eta = \frac{\text{contact width}}{a} = 2 \text{ (default)} \quad [11g]$$

$$\text{Material parameter, } \lambda_E = \frac{E'}{E_o'} \quad [11h]$$

$$\text{Geometrical parameter, } G_{LP} = d\left(\frac{1}{\sum\rho}\right)^{2-h} a^{*3-h} b^{*3-2h} \quad [11i]$$

$$\text{Cycling frequency, } u = \left|\frac{\Omega - \dot{\theta}}{\Omega_r}\right| \quad [11j]$$

$$\text{Effective elastic modulus, } \frac{1}{E'} = \frac{1-\nu_1^2}{E_1} + \frac{1-\nu_2^2}{E_2},\ E_o' = E_{52100}'. \quad [11k]$$

$\sum\rho$ is the sum of effective curvatures of the contacting surfaces in the transverse and rolling directions; E_1, ν_1, E_2, ν_2, are, respectively, the elastic modulus and Poisson's ratio of the two contacting surfaces; d is the track diameter on the race; a, b are Hertzian major and minor contact half widths; a^*, b^* are dimensionless major and minor contact half width solutions as documented by Harris and Kotzalas *(23)*; $\dot{\theta}$ is the ball orbital velocity; Ω is the race angular velocity; Ω_r is the angular velocity of the rotating race; and Φ_{LP} permits adjustment to the empirical life constant and is presently set to 1.0.

LP ball life equations

A ball in a ball bearing may have multiple tracks when the ball is subject to precession and the total number of contact cycles may be distributed over the multiple tracks; in this situation, the contact cycles have to be summed over all tracks to compute the rolling element life. Because the volume of each individual track is the same, the total effect may be closely simulated by one track with the total number of stress cycles. In addition, any details of contact distribution will be included in the constants in Eq. [7] when the life predictions are correlated to experimental life data to derive the applicable empirical constant; therefore, the details of stressed tracks may be insignificant. The LP ball life equations may now be written as

$$\frac{1}{L_{bLP}} = \left(\frac{p_H}{p_{HcbLP}}\right)^{\frac{c+2-h}{m}} \quad [12a]$$

Dynamic stress capacity,

$$p_{HcbLP} = \Phi_{bLP} A_{LP} \kappa_{LP}^{-\frac{1}{c+2-h}} \lambda_E^{\frac{2-h}{c+2-h}} G_{bLP}^{-\frac{1}{c+2-h}} u_b^{-\frac{m}{c+2-h}} \quad [12b]$$

$$\text{Geometric parameter, } G_{bLP} = D\left(\frac{1}{\sum\rho}\right)^{2-h} a^{*3-h} b^{*3-2h} \quad [12c]$$

$$\text{Cycling frequency, } u_b = \left|\frac{\omega_b - \Omega}{\Omega_r}\right|. \quad [12d]$$

ω_b is the ball angular velocity; D is the diameter of the ball; Φ_{bLP} is a future adjustment factor for the ball life constant, presently set to 1.0; and all other variables are the same as those defined for the race in Eqs. [11d] to [11k].

GZ race life equations for ball bearings

Similar to the LP formulation presented above, the point contact solutions may be substituted in the fundamental GZ equation [10] to derive the following GZ life equations:

$$\frac{1}{L_{GZ}} = \left(\frac{p_H}{p_{HcGZ}}\right)^{\frac{cm+2}{m}} \quad [13a]$$

Dynamic stress capacity,

$$p_{HcGZ} = \Phi_{GZ} A_{GZ} \kappa_{GZ}^{-\frac{1}{cm+2}} \lambda_E^{\frac{2}{cm+2}} G_{GZ}^{-\frac{1}{cm+2}} u^{-\frac{m}{cm+2}} \quad [13b]$$

$$\text{Life constant, } A_{GZ} = \left[\frac{E_o'^2}{\pi^3 K_{GZ}}\right]^{\frac{1}{cm+2}} \quad [13c]$$

$$\text{Constant, } \kappa_{GZ} = \frac{\eta \zeta_{GZ}^{cm} \xi_{GZ}}{a_1} \quad [13d]$$

$$\text{Shear stress ratio, } \zeta_{GZ} = \frac{\tau_m}{p_H} = 0.30 \text{ (default)} \quad [13e]$$

$$\text{Shear stress depth ratio, } \frac{z_m}{b} = \xi_{GZ} = 0.786 \text{ (default)} \quad [13f]$$

$$\text{Geometrical parameter, } G_{GZ} = d\frac{(a^* b^*)^3}{(\sum\rho)^2}. \quad [13g]$$

Similar to the LP equation, Φ_{GZ} is a factor for future adjustment of the life constant, and all other variables are the same as those in LP equations [11d] to [11k].

GZ ball life equations

Again, similar to the LP equations, the ball life equations are written as

$$\frac{1}{L_{bLP}} = \left(\frac{p_H}{p_{HcbLP}}\right)^{\frac{cm+2}{m}} \quad [14a]$$

Dynamic stress capacity,

$$p_{HcbGZ} = \Phi_{bGZ} A_{GZ} \kappa_{GZ}^{-\frac{1}{cm+2}} \lambda_E^{\frac{2}{cm+2}} G_{bGZ}^{-\frac{1}{cm+2}} u_b^{-\frac{m}{cm+2}} \quad [14a]$$

$$\text{Geometric parameter, } G_{bGZ} = D\frac{(a^* b^*)^3}{(\sum\rho)^2}. \quad [14b]$$

All other variables are same as those in LP equations [11d] to [11k].

Note the simplicity and generalities in both the above LP and the GZ equations. Unlike the original LP life equations, the empirical constant, A, is material independent; the properties of AISI 52100 bearing steel are only used as a scaling parameter, and the actual material properties are supplied in the newly introduced materials parameter, λ_E. The parameter κ is essentially a constant, representing the assumptions used in defining the relationship between contact pressure and critical subsurface shear stress and its depth in relation to contact half width. Rather than combining this with the base empirical constant, A, this constant is preserved as a separate term in order to maintain generality for future model refinement. The stress cycling frequency u is simply defined in terms of operating speed of the bearing. The only parameter that requires somewhat detailed contact analysis is the geometric parameter G. The contact half widths a and b require Hertzian point contact elasticity analysis. Normally, the required elasticity analysis is commonly available in any rolling bearing code that provides simple load–deflection analysis. However, when such an analysis is not available, a simplified computation, as described in Appendix A, may be used to implement the above life equations.

LP race life equations for roller bearings

After substituting the line contact solution, as summarized in Appendix A, in the LP fundamental equation [7], the race life at each roller to race contact is written as

$$\frac{1}{L_{LP}} = \left(\frac{\overline{p}_H}{\overline{p}_{HcLP}}\right)^{\frac{c-h+1}{m}} \quad [15a]$$

Dynamic stress capacity,

$$\overline{p}_{HcLP} = \overline{\Phi}_{LP} B_{LP} \kappa_{LP}^{-\frac{1}{c-h+1}} \lambda_E^{\frac{1-h}{c-h+1}} \overline{G}_{LP}^{-\frac{1}{c-h+1}} u^{-\frac{m}{c-h+1}} \quad [15b]$$

$$\text{Life constant, } B_{LP} = \left(\frac{2^{h-1}}{\pi E_o^{'h-1} K_{LP}}\right)^{\frac{1}{c-h+1}} \quad [15c]$$

$$\text{Geometric parameter, } \overline{G}_{LP} = \frac{da}{(\sum\rho)^{1-h}}. \quad [15d]$$

Again, similar to the point contact equations, $\overline{\Phi}_{LP}$ is an adjustment factor for future use, presently set equal to 1.0. All other variables are the same as those defined in LP point contact equation [11d] to [11k].

LP roller life equations

Similar to the point contact equations, the roller life equations are essentially the same as the race equations, except that the track diameter is set equal to the roller diameter and the contact frequency is changed to u_b, Eq. [12d].

$$\frac{1}{L_{bLP}} = \left(\frac{\overline{p}_H}{\overline{p}_{HcbLP}}\right)^{\frac{c-h+1}{m}} \quad [16a]$$

Dynamic stress capacity,

$$\overline{p}_{HcbLP} = \overline{\Phi}_{bLP} B_{LP} \kappa_{LP}^{-\frac{1}{c-h+1}} \lambda_E^{\frac{1-h}{c-h+1}} \overline{G}_{bLP}^{-\frac{1}{c-h+1}} u_b^{-\frac{m}{c-h+1}} \quad [16b]$$

$$\text{Geometric parameter, } \overline{G}_{bLP} = \frac{Da}{(\sum\rho)^{1-h}}. \quad [16c]$$

All other parameters are the same as those defined earlier for LP point contact equations [11d] to [11k].

GZ race life equations for roller bearings

For the GZ model, the elastic line contact solutions are substituted in the fundamental equation [10] to arrive at the following race life equation:

$$\frac{1}{L_{GZ}} = \left(\frac{\overline{p}_H}{\overline{p}_{HcGZ}}\right)^{\frac{cm+1}{m}} \quad [17a]$$

Dynamic stress capacity,

$$\overline{p}_{HcGZ} = \overline{\Phi}_{GZ} B_{GZ} \kappa_{LP}^{-\frac{1}{cm+1}} \lambda_E^{\frac{1}{cm+1}} \overline{G}_{GZ}^{-\frac{1}{cm+1}} u^{-\frac{m}{cm+1}} \quad [17b]$$

$$\text{Life constants, } B_{GZ} = \left(\frac{E_o^{'}}{2\pi K_{GZ}}\right)^{\frac{1}{cm+1}} \quad [17c]$$

$$\text{Geometric parameter, } \overline{G}_{GZ} = \frac{da}{\sum\rho}. \quad [17d]$$

All other variables are the same as those defined earlier for LP point contact equations [11d] to [11k].

GZ roller life equations

For the roller, the GZ life equations are

$$\frac{1}{L_{bGZ}} = \left(\frac{\overline{p}_H}{\overline{p}_{HcbGZ}}\right)^{\frac{cm+1}{m}} \quad [18a]$$

Dynamic stress capacity,

$$\overline{p}_{HcbGZ} = \overline{\Phi}_{GZ} B_{GZ} \kappa_{LP}^{-\frac{1}{cm+1}} \lambda_E^{\frac{1}{cm+1}} \overline{G}_{bGZ}^{-\frac{1}{cm+1}} u_b^{-\frac{m}{cm+1}} \quad [18b]$$

$$\text{Geometric parameter, } \overline{G}_{bGZ} = \frac{Da}{\sum\rho}. \quad [18c]$$

All other parameters are the same as those defined earlier for LP point contact equations [11d] to [11k].

All of the above relations compute life as a function of contact stress. In the event that life relations are desired in terms of load, as implemented in the original LP model, these relations can be easily converted to load-based relations based on the relationship between load and stress for both point and line contacts. The resulting equations are summarized in Appendix B.

Note that in the above generalized formulations for both point and line contacts, the empirical constants and the various exponents may be varied independently. This permits greatly improved life modeling with different race and rolling element materials, such as hybrid bearings where the stress life exponents for ceramic rolling elements may be different.

Relation between ball and roller bearing constants

Because the fundamental equations [7] and [10], for the LP and GZ models, respectively, apply to both point and line contacts, the constants in point and line contact life equations, developed above, are related. This is noted by comparing the constants A_{LP} and B_{LP} in Eqs. [11c] and [15c] and A_{GZ} and B_{GZ} in Eqs. [13c] and [17c]. Elimination of K_{LP} in Eqs. [11c] and [15c] provides the following relationship between the point and line contact LP constants:

$$B_{LP} = \left[\frac{\pi^{2-h}}{2^{1-h}} \frac{A_{LP}^{c-h+2}}{E_o'}\right]^{\frac{1}{c-h+1}}. \quad [19]$$

Likewise, elimination of K_{GZ} in Eqs. [13c] and [17c] provides the following relationship between the GZ point and line constants:

$$B_{GZ} = \left[\frac{\pi^2}{2} \frac{A_{GZ}^{cm+2}}{E_o'}\right]^{\frac{1}{cm+1}}. \quad [20]$$

Lundberg and Palmgren *(7), (8)*, after carrying out a correlation analysis of a relatively large amount of experimental data, have suggested the values of 31/3 and 7/3 for the exponents c and h, respectively. The values for Weibull slope or modulus, m, have been suggested as 10/9 and 9/8 for point and line contacts, respectively. These values yield load life exponents of 3 and 4 for point and line contacts, respectively. However, a difference in Weibull modulus between point and line contacts provides unrelated values for the point and line contact constants.

In the present work, in order to maintain the validity of fundamental life equations [7] and [10] for both point and line contacts, the Weibull slope is set to 10/9 in both point and line contacts, along with the suggested values of exponents c and h. This yields a load life exponent of 3 for point contacts and 4.05 for line contacts. It is expected that this small difference in the load life exponents is well within the statistical variance in Weibull modulus when estimated from experimental data. The current analysis is, of course, in terms of stress, where the corresponding values of Hertz stress life exponents will be 9 and 8.10 for point and line contacts, respectively.

Practical significance of maintaining the relationship between point and line contacts leads to the convenient fact that once the life constant is estimated for ball bearings, the applicable constant for roller bearings is also established. In the current work, the point contact constant is estimated from the available ball bearing life data and then the applicable roller bearing constant is estimated from the above relationship.

Life equations for complete bearing

All of the above life equations provide estimates of life at each contact in the bearing. In order to estimate the life of the bearing as a whole, these lives have to be statistically summed. If only one of the races rotates in the bearing, then for the stationary race, each individual contact is independent of each other and, thus, if the number of rolling elements in the bearing is n, then the life of the stationary race, L_s, may be written as

$$\frac{1}{L_s} = \left[\sum_{j=1}^{n} \left(\frac{1}{L_j}\right)^m\right]^{1/m}. \quad [21]$$

For the rotating race, each contact goes through the same cyclic load variation; thus, for the rotating race, all contact lives may be simply summed together, which yields the life of the rotating race, L_r, as

$$\frac{1}{L_r} = \sum_{j=1}^{n} \frac{1}{L_j}; \quad [22]$$

for the rotating rolling element, the lives at the outer and inner race contacts are simply summed to get the rolling element life

$$\frac{1}{L_{re}} = \sum_{i=1}^{2} \frac{1}{L_{rei}}. \quad [23]$$

For the entire bearing, the lives of both races and rolling elements may be statistically summed together, using strict series reliability (Zaretsky *(19)*), as

$$\frac{1}{L_{brg}} = \left\{\left(\frac{1}{L_s}\right)^m + \left(\frac{1}{L_r}\right)^m + \sum_{j=1}^{n} \left(\frac{1}{L_{rej}}\right)^m\right\}^{1/m}. \quad [24]$$

For the present investigation, the above analytical formulation is implemented in bearing dynamic model ADORE (Gupta *(22)*) to generate all of the parametric results, although all of the above equations may be easily implemented in any bearing life modeling computer code. In fact, the linearized point contact solutions, as summarized in Appendix A, permit model implementation without much need for any sophisticated computing resource.

Table 1. Summary of selected NASA endurance tests with 120-mm-bore angular-contact ball bearings at temperatures from 478 to 588 K and speeds to 3 million DN.

Data set (reference)	Bearing material	Operating temperature (K)	Thrust load (N)	Shaft speed (rpm)	Lubricant	Failure index	Estimated basic L_{10} life (h)
Set 1 (Zaretsky, et al. *(24)*)	CEVM AISI M50	478	25,800	12,000	PAO	10/27	30.10
Set 2 (Zaretsky *(25)*)	CEVM AISI M50	492	25,800	12,000	PAO	14/27	15.66
Set 3 (Zaretsky, et al. *(24)*)	CEVM AISI M50	533	25,800	12,000	PAO	11/26	25.30
Set 4 (Zaretsky, et al. *(24)*)	CEVM AISI M50	589	25,800	12,000	PAO	6/26	33.33
Set 5 (Bamberger, et al. *(26)*)	VIMVAR M50	492	22,400	25,000	MIL-L-23699	6/30	50.40

Results and discussion

Experimental life data and correlation for model constants

The available experimental life data for derivation of model constants and validation of the newly developed models is very limited. The data generated prior to 1940, used by Lundberg and Palmgren *(6), (7)* to develop the original life models, were never published in the open literature. A decade later, with significant advancement in materials technology, the NASA Lewis Research Center (now NASA Glenn Research Center) undertook a major bearing life testing initiative, using elemental bearing bench testers and full-scale rolling element bearing endurance testing (Zaretsky, et al. *(24)*; Zaretzky *(25)*) at bearing operating conditions to temperatures up to 589 K (600°F) and bearing operating speeds to 3 million DN (product of bearing bore in millimeters and shaft revolutions per minute; Bamberger, et al. *(26)*). Some of these tests included the first use of vacuum induction melted–vacuum arc remelted (VIM-VAR) AISI M-50 steel. Subsequent to this work, because there are no other life data presently available in the public domain, the NASA data sets are used in the current investigation to derive the model constants. However, because the newly generalized life models contain discrete materials parameters and the new stress capacity equations provide an adjustment factor for future use, recalibration of the model constants, as newer data become available, is quite straightforward.

The current work uses five of the NASA data sets, as summarized in Table 1. These data sets were also used recently by Gupta, et al. *(20)*. The failure index in Table 1 denotes the number of bearings failed out of the total number tested. The indicated basic L_{10} life is derived by first carrying out the Weibayes analysis, with a prescribed Weibull dispersion of 1.1111, to estimate 90% survival life; then this life is divided by the applicable materials and lubrication factors as documented by Gupta, et al. *(20)*.

For the first four of these data sets (Zaretsky, et al. *(24)*; Zaretsky *(25)*), the test bearings were ABEC-5 grade, split inner-race, 120-mm-bore angular-contact ball bearings with nominal geometry summarized in Table 2. All bearings in these four data sets operated with a thrust load of 25,800 N (5,800 lbf) at 12,000 rpm (1.44 DN). The material for the balls and inner and outer races was consumable-electrode vacuum-melted (CEVM) AISI M-50 steel. The retained austenite contents of the ball and race materials were less than 3%. The nominal Rockwell C hardness of the balls and races was 63 at room temperature. The cage was a one-piece outer land riding type made of a nickel base alloy (AMS-4892) with a nominal Rockwell C hardness of 33. All components with the exception of the cage were matched for hardness within 0.5 point Rockwell C. This matching assured a nominal differential hardness (the ball hardness minus the race hardness) commonly called ΔH, of 0 in all bearings. The surface finishes of the balls and raceways were 2.5 μcm (1 μin.) and 5 μcm (2 μin.) AA respectively. The bearings were jet lubricated with poly-alpha-olefin (PAO).

Data set 5 corresponds to the 3 million DN tests (Bamberger, et al. *(26)*). The bearings again were ABEC-5 grade, but the material for both the balls and races was double vacuum-melted VIM-VAR AISI M-50 steel, for which an approximately 15% reduction in elastic modulus was reported at the indicated temperature *(27)*. This was the first use of VIM-VAR AISI M-50 steel for bearings. Bearing geometry was identical to that summarized in Table 2, except that the contact angle was changed to 24° primarily to accommodate increased centrifugal expansion of the inner race at high speed. All bearings in this data set operated at 25,000 rpm (3 million DN) with a thrust load of 22,400 N (5,000 lbf). Nominal hardness of the balls and races was Rockwell C-63 at room temperature. The retained austenite content of the balls and races was less than 3%. The cage was a one-piece inner land riding type, made out of an iron base alloy (AMS 6415) heat-treated to a Rockwell C hardness range of 28–35 and with a 0.005-cm (0.002-in.) maximum thickness of silver plate (AMS 2410). The cage was balanced within 3 g-cm (0.042 oz.-in.). The bearing was underrace lubricated, with MIL-L-23699 lubricant, via radial holes machined into the halves of the split inner race.

Table 2. Ball bearing geometry.

Bearing bore	120 mm	Pitch diameter	155 mm
Bearing outer diameter	190 mm	Contact angle	20°
Number of balls	15	Outer race curvature factor	0.52
Ball diameter	20.6375 mm	Inner race curvature factor	0.54

Table 3. Estimated model constants derived from least-squared deviation analysis of experimental life data.

LP shear stress exponent, $c = \frac{31}{3}$
LP depth exponent, $h = \frac{7}{3}$
LP Weibull dispersion, $m = \frac{10}{9}$
Effective contact width to major half width ratio, $\eta = 2$

Model constant	LP model	GZ model
Failure shear stress (maximum orthogonal for LP and maximum for GZ) to contact pressure ratio	$\zeta_{LP} = 0.25$	$\zeta_{GZ} = 0.30$
Depth of failure shear stress to contact half width ratio	$\xi_{LP} = 0.50$	$\xi_{GZ} = 0.786$
Point contact stress–based constant	$A_{LP} = 1.4599 \times 10^9$ N/m$^{1.933}$	$A_{GZ} = 6.4229 \times 10^8$ N/m$^{1.777}$
Point contact stress life exponent	9.00	12.133
Line contact stress–based constant	$B_{LP} = 9.6020 \times 10^8$ N/m$^{1.926}$	$B_{GZ} = 4.8376 \times 10^8$ N/m$^{1.760}$
Line contact stress life exponent	8.100	11.233

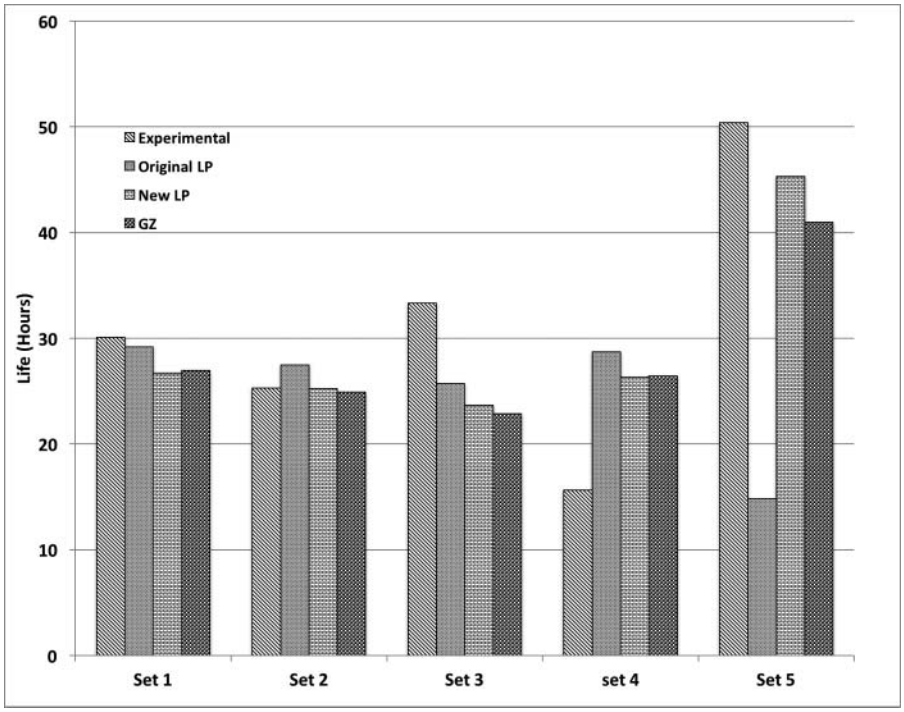

Figure 1. Comparison of predicted lives with experimental life data for the five data sets summarized in Table 1.

Provision was also made for inner race land-to-cage lubrication, by the incorporation of several small-diameter holes radiating from the bore of the inner race to the center of the inner race shoulder. The OD of the outer race was oil cooled.

A least-squared deviation analysis was used to fit the life models to these data sets and derive the point contact model constant with the Lundberg-Palmgren values of the exponents *c*, *h*, and *m*. Once this constant is estimated, the constant for line contacts is estimated by using Eqs. [19] and [20] for the LP and GZ models, respectively. Computed values of these constants along with the other constants for both life models are summarized in Table 3.

A comparison of predicted lives against the experimental lives obtained with each of the five sets is presented in Fig. 1. For reference, life predictions of the original Lundberg-Palmgren model are also reproduced from Gupta, et al. *(20)*. For data sets 1 to 4, clearly all of the models agree fairly well with the experimental data. For set 5, however, the original LP life is significantly lower than the experimental life, whereas the new LP and the GZ lives are much closer to the experimental life. The higher life in data set 5 is primarily attributed to significant reduction in elastic modulus of the VIM-VAR AISI M50 bearing steel at the operating temperature of 492 K. The original LP model does not permit variation in elastic modulus, and the life is based on a constant modulus of AISI 52100 bearing steel. As a result, the model fails to simulate the increase in life due to a reduction in modulus with increasing temperature. The parametric results presented below further elaborate on the significance of variation in elastic properties in life predictions.

Ball bearing parametric results

In order to further elaborate the differences between the LP and the newly introduced GZ life models, parametric life results are obtained with the 120-mm-bore angular-contact ball bearing corresponding to experimental data set 5, discussed above. The bearing geometry was summarized in Table 2 with the exception that the contact angle is 24°, as applicable to experimental data set 5. For a valid comparison with the original LP model, the bearing material is set to AISI 52100. Parametric life results are obtained as a function of contact stress with the bearing operating at room temperature at a speed of 17,000 rpm (2.04 million DN). The elastic modulus thus corresponds to that of AISI 52100 bearing steel at room temperature. For the newly developed LP model, the results are shown in Fig. 2; the computed lives of both races, rolling elements, and the entire bearing are plotted along with the bearing life as predicted by the widely used original LP model. For the purpose of discussion, "LP model" refers to the new stress-based LP model developed in this article and "original LP model" refers to the commonly used load-based LP model. Clearly, under the current room temperature conditions with the AISI 52100 bearing steel, the bearing life predicted by the newly developed LP model is identical to that predicted by the original model as expected. In fact, the two curves are essentially on top of each other.

With the GZ model, the predicted life is higher compared to the LP model at low stresses and lower at very high stresses; this is primarily due to a higher stress-life exponent inherent in the GZ model. The results are shown in Fig. 3. For comparison purposes, the life predicted by the new LP model is reproduced here from Fig. 2.

The ratio of the GZ to LP life seems to approach a constant value as the contact stress reduces to very low values, and the ratio constantly reduces in the very high stress range; the lives as predicted by the two models are essentially identical in the range of 2 to 3 GPa. Because the bearing considered in the above evaluation is operating at relatively

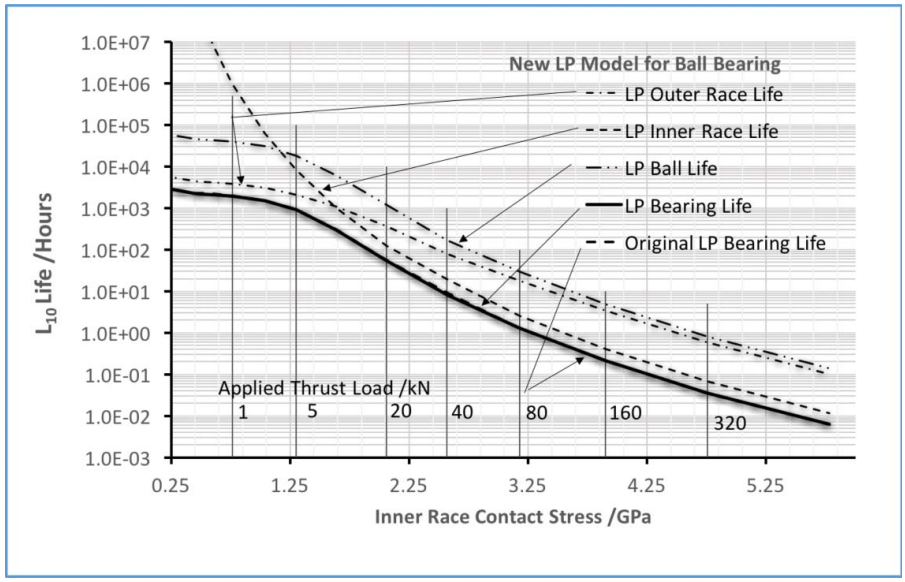

Figure 2. Life predictions with the new LP model for the 120-mm angular-contact ball bearing operating at 17,000 rpm at room temperature.

high speed, the balls maintain contact with the outer race under high centrifugal force, and the inner race is significantly unloaded as the applied load continues to reduce. Thus, though the outer race and ball lives stabilize to fairly constant values, the life of the inner race keeps increasing as the applied load, or inner race contact stress, continues to reduce. Therefore, as the inner race contact stress reduces, both the GZ and LP lives stabilize to constant values, which results in a constant value of life ratio at very low loads. Figure 4 plots the GZ-to-LP life ratio as a function of inner race contact stress at different operating speeds. Clearly, the ratio of GZ to LP life at low stresses progressively increases as the operating speed decreases; at very low speeds, when the contact stresses are low at both inner and outer races, the life ratio increases by several orders of magnitude. These high values of lives predicted by the GZ model may be very comparable to the infinite lives predicted by the limiting shear stress models (Ioannides and Harris *(15)*).

To complement the parametric results presented in Fig. 4, the corresponding outer race contact stress is plotted in Fig. 5. As the applied load or inner race contact stress is reduced, the outer race contact stress approaches a constant value corresponding to the centrifugal force applicable at the operating speed. The stress is, of course, higher at higher speeds, which results in reducing life with increasing speed as demonstrated in Fig. 4.

Further practical significance of the newly developed models is seen when the elastic modulus of the bearing materials differs from that of the AISI 52100 bearing steel, on which the widely used original LP model is based. For this purpose, the bearing material of the 120-mm angular-contact ball bearing was changed to VIM-VAR AISI M50 bearing steel, for which the elastic modulus drops with increasing temperature *(27)*, and life simulations were carried out as a function of temperature with a thrust load of 10,000 N and shaft speed of 17,000 rpm. The applicable variation of the materials parameter λ_E as a

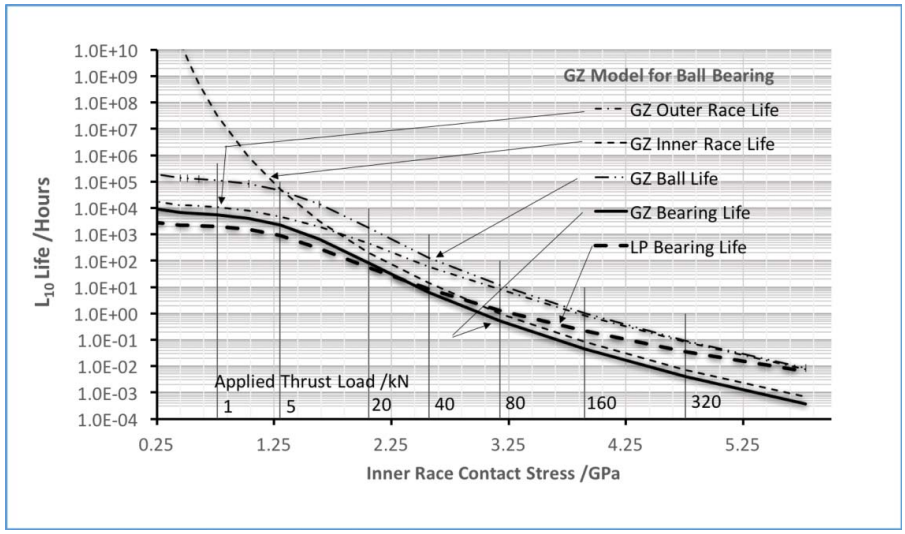

Figure 3. GZ life predictions compared with the LP predictions for the 120-mm angular-contact ball bearing operating at 17,000 rpm at room temperature.

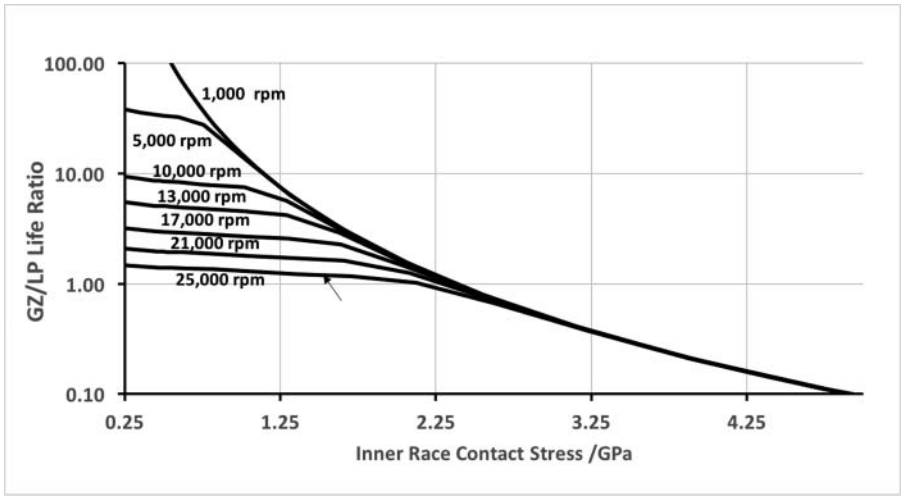

Figure 4. The GZ and LP life ratio as a function of contact stress and operating speed.

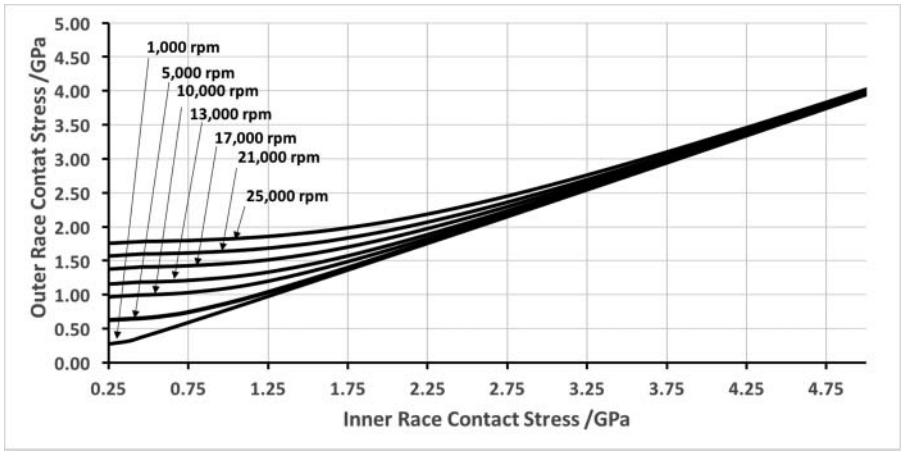

Figure 5. Outer race contact stress as a function of inner race contact stress at varying operating speeds.

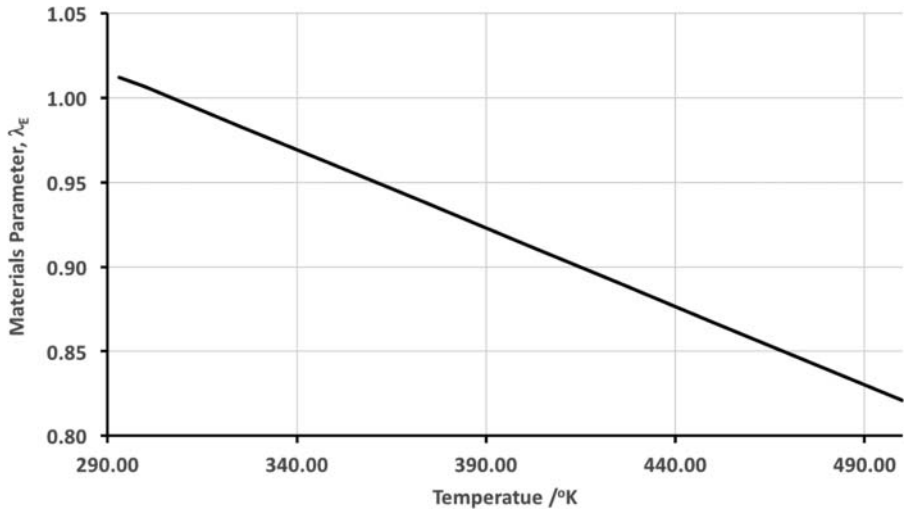

Figure 6. Variation in materials parameter as a function of temperature for the VIM-VAR AISI M50 bearing steel.

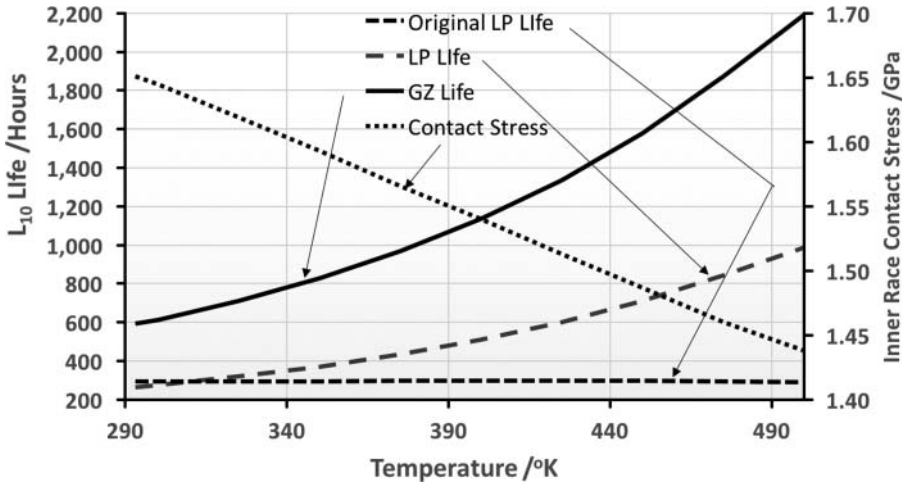

Figure 7. Predicted lives with various life models as a function of operating temperature.

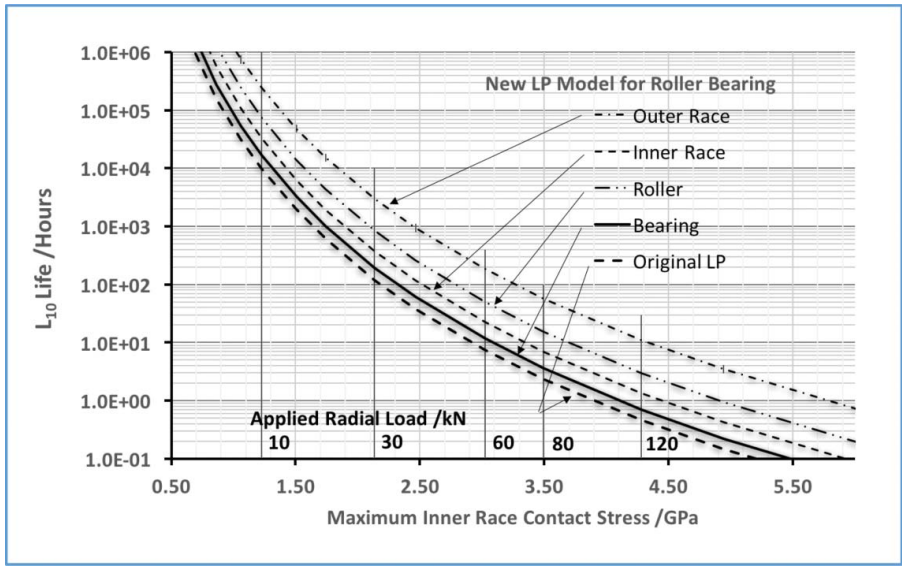

Figure 8. Comparison of predicted life with the new and original LP models for an ANSI 52100 steel, 210-size cylindrical roller bearing operating at 10,000 rpm at room temperature.

function of temperature is shown in Fig. 6, and the resulting effect on bearing life as predicted by the various models is shown in Fig. 7.

Both the newly developed LP and the GZ models show increasing life with increasing temperature as a result of reducing elastic modulus. The drop in contact stress due to reducing modulus is also shown in Fig. 7. This figure also shows the life predicted by the original LP model, where the basic life constant includes the properties of AISI 52100 bearing steel and the life equation does not have any elastic modulus parameter; the predicted life is insensitive to temperature. Small changes in contact (Hertz) stresses due to thermal and centrifugal distortions are fully accounted for in all of the models; however, this change is insignificant in comparison to the change in Hertz stress due to the reduction in elastic modulus. More recent measurements of elastic properties of AISI 52100 bearing steel have also shown drop in elastic modulus as a function of temperature (Guo and Liu *(28)*).

Table 4. Cylindrical roller bearing geometry.

Bearing bore	50 mm	Number of rollers	14
Bearing outer diameter	90 mm	Roller length	13 mm
Roller diameter	13 mm	Pitch diameter	70.65 mm

Roller bearing parametric results

As discussed earlier, the roller bearing life constant is computed from the one validated for ball bearings, and parametric life results are obtained for a 210-size cylindrical roller bearings. The nominal bearing geometry is documented in Table 4. For this investigation, the roller surface has no crown and the effective length of the contact is equal to the roller length.

The bearing material was again set to AISI 52100 bearing steel for valid comparison with the original LP model, and life simulations were obtained as a function of contact stress at 10,000 rpm

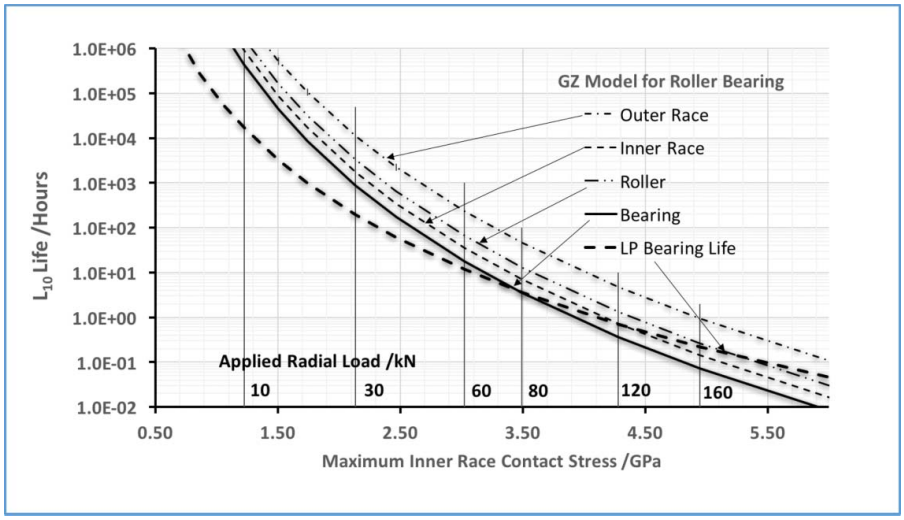

Figure 9. Parametric life results with the GZ model for a AISI 52100 steel, 210-size cylindrical roller bearing, operating at 10,000 rpm at room temperature, compared with the new LP model.

under room temperature conditions. The mounted internal clearance was arbitrarily set to zero, primarily to demonstrate the role of centrifugal expansion of the rotating inner race as a function of speed. Thus, under no applied load, all of the rollers are touching both races. The parametric race, roller, and bearing lives are shown in Fig. 8 for the newly developed LP model along with the life predictions by the original LP model, as documented by Harris and Kotzalas *(23)*. The life predictions with the new LP model are slightly higher than those provided by the original model; the ratio of new to original LP life is about 1.4 at very high stress and about 2 at very low stress. This difference corresponds to a maximum discrepancy of about 8% in the dynamic stress capacity. This small difference can be easily explained in terms of a slightly higher stress life exponent resulting from Weibull dispersion of 1.1111 in comparison to 1.125 used in the original LP model for roller bearings. In addition, this 8% difference in stress capacity may be insignificant in comparison with normal scatter in experimental life data.

Corresponding parametric results for the GZ model are shown in Fig. 9. Again the GZ lives are significantly higher at low stresses. The crossover in life in relation to the LP model appears at a slightly higher stress, in comparison to that seen in Fig. 3 for ball bearings.

Unlike the angular-contact ball bearing, where the contact angles and stresses at the outer and inner race contacts change with load and speed, the contact between roller and races in a radially loaded cylindrical roller bearing is always in the radial direction, and depending on the initial internal clearance and operating speed, the rollers maintain contact with the inner race due to centrifugal expansion or the rotating inner race. To demonstrate this effect, the initial mounted internal clearance in the bearing is set to zero. Thus, as the bearing rotates under no applied load, only the centrifugal expansion of the inner race loads all of the rollers with both races. The life will be reduced as the speed increases due to increasing stresses.

Because the GZ model yields significantly higher lives at light loads, the GZ-to-LP life ratio becomes quite large at low speeds. This is demonstrated in Fig. 10, where the life ratio is plotted as a function of maximum inner race contact stress at varying operating speeds. Note that as the operating speed increases and the applied radial load is reduced to zero, the inner race contact stress does not go to zero; instead, it approaches a constant value determined by the centrifugal expansion of the inner race and the centrifugal force on the roller. Thus, the solutions in Fig. 10 do not extend to zero inner race contact stress as the operating speed increases.

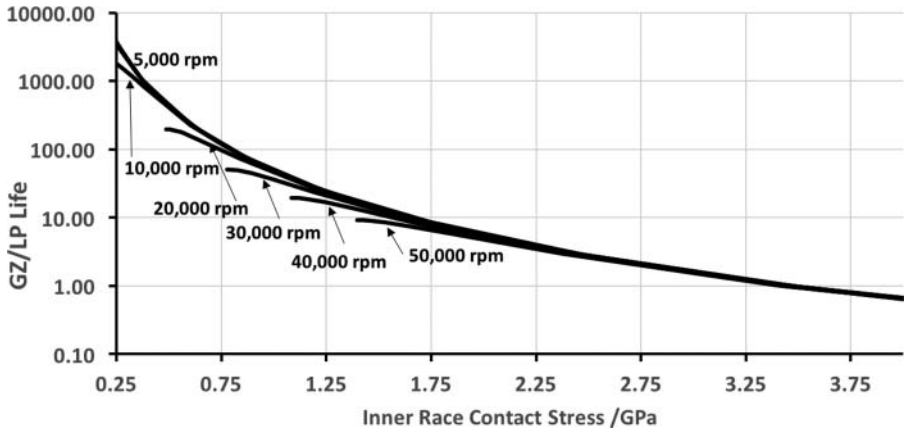

Figure 10. The GZ-to-LP life ratio as a function of contact stress and operating speed for the 210-size cylindrical roller bearing.

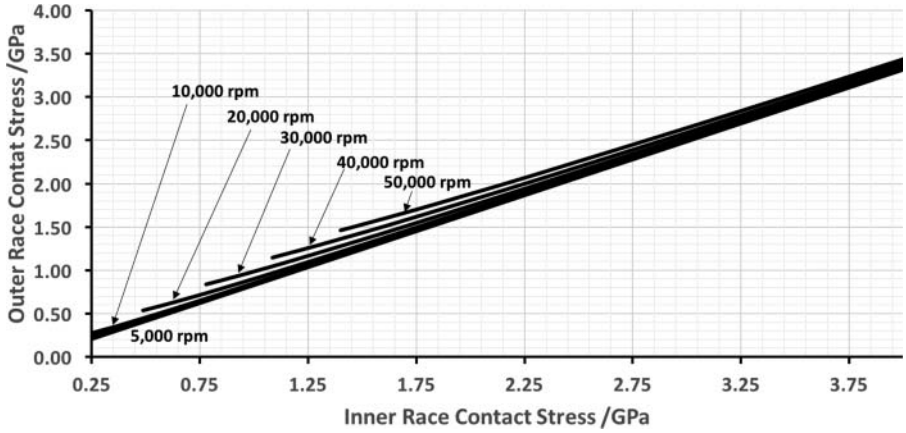

Figure 11. Outer and inner race contact stresses at varying operating speeds in the 210-size cylindrical roller bearing.

The corresponding outer race contact stress is shown in Fig. 11. Again, at very low applied load, the stresses at both the outer and inner race contacts approach a constant value corresponding to the operating speed and initial internal clearance in the bearing. Because minimum stress is defined when the applied external load is zero and the roller contact is maintained by the centrifugal load on the roller, the centrifugal expansion of the inner race, and the initial internal clearance in the bearing, the solutions do not extend to zero inner race stress.

Summary of results

This investigation introduces two new fatigue life models for rolling bearings. First, the commonly used LP model is generalized to introduce a new dynamic stress capacity relation with discrete geometrical and materials parameters so that the empirical constant is now independent of material properties. Secondly, based on earlier work, a new GZ model is introduced that also relates life to contact stress with distinct geometrical and materials parameters. Both the newly developed models provide life equations for independent computation of life of races and rolling elements at each contact. These contact lives are then statistically summed to estimate lives of the races, rolling elements, and the complete bearing. The empirical constants for both models were derived by a regression analysis of available experimental life data. The following results were obtained by carrying out a parametric evaluation of both models:

1. For a ball bearing with AISI 52100 bearing steel, the properties of which are included in the original Lundberg-Palmgren model, life predictions with the newly developed LP model are identical to those provided by the original LP model.
2. Similar to the dynamic load capacity in the currently used models, the new formulations relate bearing life to a newly defined dynamic stress capacity.
3. Unlike the model constants in the currently used original Lundberg-Palmgren models, the model constants in the new formulations are independent of material properties. Thus, application to either different materials or materials where the properties vary with operating temperature is more precisely accomplished.
4. The empirical constants in the stress capacity equations for point and line contacts are related to the constant in the fundamental life equation applicable to both point and line contacts. Thus, if the empirical constant for a point contact equation is developed by correlating experimental ball bearing life data to model predictions, then the constant for line contact equation, as applicable to roller bearings, is also defined.
5. Comparison of parametric lives, as predicted by the LP and GZ models, show that while in the operating range of 2 to 3 GPa contact stress the life estimates are closely similar, the GZ model provides significantly higher lives at low stresses. At very high stress levels, above 3 GPa for ball bearings and above 4 GPa for roller bearings, the GZ lives are lower than the LP-predicted lives.

In the future, it is expected that the newly introduced stress-based life models will provide easier implementation of residual stresses, as applicable to case-hardened materials, and the hoop stresses in high-speed bearings. In addition, by relating the materials and geometrical parameters to operating temperature, bearing life predictions may be better integrated with the thermal interactions in the bearing.

Acknowledgments

Work reported in this article was sponsored by the United States Air Force under Small Business Innovation Research (SBIR) Phase I (Contract #FA8650-13-M-2406) and Phase II (Contract #FA8650-15-C-2534) contracts awarded to PKG Inc. The Air Force Technical Contract Monitors were Captain Justin Mason, Captain Ryan Kolesar and Jeremy Nickell.

References

(1) Harris, T. A. (1991), *Rolling Bearing Analysis*, 3rd ed., John Wiley & Sons: New York, pp 6.
(2) Tallian, T. (1969), *Progress in Rolling Contact Technology*, SKF Industries, Inc.: King of Prussia, PA.
(3) Palmgren, A. (1924), "Die Lebansdauer von Kugellagern" [The Service Life of Ball Bearings], *Zeitschrift des Vereines Deutscher Ingenieure*, **68**(14), pp 339–341.
(4) Zaretsky, E. V. (1998), "A. Palmgren Revisited—A Basis for Bearing Life Prediction," *Lubrication Engineering*, **54**(2), pp 18–24.
(5) Weibull, W. (1939), "A Statistical Theory of the Strength of Materials," *Inginiors Vetenskaps Adademien*, **151**.
(6) Weibull, W. (1939), "The Phenomenon of Rupture," *Inginiors Vetenskaps Adademien*, **153**.
(7) Lundberg, G. and Palmgren, A. (1947), "Dynamic Capacity of Rolling Bearings," *Acta Polytech., Mech. Eng.*, Series 1, No 3, 7, Royal Swedish Acad. Eng.

(8) Lundberg, G. and Palmgren, A. (1952), "Dynamic Capacity of Roller Bearings," *Acta Polytech. Mech. Eng.*, Series 2, No. 4, 96, Royal Swedish Acad. Eng. 6.
(9) ANSI/AFBMA 9:1990 (R2000). (2000), "Load Rating and Fatigue Life for Ball Bearings," The Anti-Friction Bearing Manufacturers Association: Washington, DC.
(10) ANSI/AFBMA 11:1990 (R2008). (2008), "Load Rating and Fatigue Life for Roller Bearings," The Anti-Friction Bearing Manufacturers Association: Washington, DC.
(11) ISO 281:2007. (2007), "Rolling Bearings—Dynamic Load Ratings and Rating Life," International Organization for Standardization: Geneva.
(12) Zaretsky, E. V. (1997), "Rolling Bearing and Gear Materials," *Tribology for Aerospace Applications*, Zaretsky, E. V. (Ed.), STLE SP-37, pp 325–451, Society for Tribologists and Lubrication Engineers: Park Ridge, IL.
(13) Zaretsky, E. V. (1992), *STLE Life Factors for Rolling Bearings*, Society for Tribologists and Lubrication Engineers: Park Ridge, IL.
(14) Tallian, T. E. (1999), "A Data-Fitted Rolling Bearing Life Prediction Model for Variable Operating Conditions," *Tribology Transactions*, **42**, pp 241–249.
(15) Ioannides, E. and Harris, T. A. (1985), "New Fatigue Life Model for Rolling Bearings," *Journal of Lubrication Technology*, **107**(3), pp 367–378.
(16) Shimizu, S. (2002), "Fatigue Limit Concept and Life Prediction Model for Rolling Contact Machine Elements," *Tribology Transactions*, **45**(1), pp 39–46.
(17) Zaretsky, E. V. (2010), "In Search of a Fatigue Limit: A Critique of ISO Standard 281:2007," *Tribology & Lubrication Technology*, **66**(8), pp 30–40.
(18) Zaretsky, E. V. (1987), "Fatigue Criterion to System Design, Life and Reliability," *AIAA Journal of Propulsion and Power*, **107**(3), pp 76–83.
(19) Zaretsky, E. V. (2002), "Rolling Bearing Life Prediction, Theory and Application," *Recent Developments in Wear Prevention, Friction and Lubrication*, Nikas, G. K. (Ed.), Research Signpost; Kerala, India, pp 45–136.
(20) Gupta, P. K., Oswald, F. B., and Zaretsky, E. V. (2012), "Comparison of Models for Rolling Bearing Dynamic Capacity and Life," *Tribology Transactions*, **58**(6), pp 1039–1053.
(21) DellaCorte, C. (2014), "Novel Super-Elastic Materials for Advanced Bearing Applications," *Advances in Science and Technology*, **89**, pp 1–9.
(22) Gupta, P. K. (1984), *Advanced Dynamics of Rolling Elements*, Springer-Verlag: New York.
(23) Harris, T. A. and Kotzalas, M. N. (2007), *Rolling Bearing Analysis—Fifth Edition—Essential Concepts of Bearing Technology*, CRC Press: Boca Raton, FL.
(24) Zaretsky, E. V., Anderson, W. J., and Bamberger, E. N. (1969), "Rolling-Element Bearing Life from 400° to 600°F," **NASA TN D-5002**.
(25) Zaretsky, E. V. (1972), "Advanced Airbreathing Engine Lubricants Study with a Tetraester Fluid and a Synthetic Paraffinic Oil at 492 K (425°F)," **NASA TN D-6771**.
(26) Bamberger, E. N., Zaretsky, E. V., and Signer, H. (1976), "Endurance and Failure Characteristics of Main-Shaft Jet Engine Bearing at 3 × 10^6 DN," *Journal of Lubrication Technology*, **98**, pp 580–585.
(27) Material Data Sheet. Latrobe Lescalloy, M-50 VIMVAR. (2008, February) Available at: http://www.matweb.com (accessed 31 August 2016).
(28) Guo, Y. B. and Liu, C. R. (2002), "Mechanical Properties of Hardened AISI 52100 Steel in Hard Machining Processes," *Journal of Manufacturing Science and Engineering*, **124**, pp 1–9.

Appendix A—Simplified point and line contact elastic solutions

Point contact solutions

For the point contact configuration, applicable to ball bearings, based on the Hertzian elastic point contact solution, as documented by Harris and Kotzalas *(23)*, the relationships between the applied contact load, Q, and the contact pressure, p_H, and the elliptical contact half widths, a and b, respectively, are written as

$$Q = \frac{2}{3}\pi abp_H \qquad \text{[A1a]}$$

$$a = a^*\left[\frac{3}{2\sum\rho}\frac{Q}{E'}\right]^{1/3} \qquad \text{[A1b]}$$

$$b = b^*\left[\frac{3}{2\sum\rho}\frac{Q}{E'}\right]^{1/3} = a^*b^{*2}\frac{\pi}{\sum\rho}\frac{p_H}{E'} \qquad \text{[A1c]}$$

$$ab = (a^*b^*)^3\left[\frac{\pi}{\sum\rho}\frac{p_H}{E'}\right]^2 \qquad \text{[A1d]}$$

$$\frac{1}{E'} = \frac{1-\nu_1^2}{E_1} + \frac{1-\nu_2^2}{E_2}. \qquad \text{[A1e]}$$

where $\sum\rho$ is the sum of effective curvatures of the contacting surfaces in the transverse and rolling directions; E_1, ν_1, E_2, ν_2, are, respectively, the elastic modulus and Poisson's ratio of the two contacting surfaces; and a^* and b^* are dimensionless half-width solutions, which are solved by solving elliptical integrals as a function of the ellipticity ratio a/b.

For the development of stress-based life equations, the contact load, Q, in Eqs. [A1a] to [A1d] may be eliminated to express the contact half-widths in terms of contact pressure, the dimensionless solutions, a^* and b^*, geometry of the bearing elements, and elastic properties of the contacting elements.

By solving the appropriate elliptical integrals, Harris and Kotzalas *(23)* have tabulated the dimensionless solutions, a^* and b^*, as a function of the of curvature function, $F(\rho)$, which is defined as

$$F(\rho) = \frac{\rho_{11} - \rho_{12} + \rho_{21} - \rho_{22}}{\rho_{11} + \rho_{12} + \rho_{21} + \rho_{22}}, \qquad \text{[A2]}$$

where the first subscript on the curvature corresponds to either the rolling (= 1) or the transverse direction (= 2), and the second subscript corresponds interacting solids 1 and 2. Figure A1 shows the solutions for a^*, b^*, a^*/b^*, and a^*b^* in graphic form. The geometrical parameter, G, in the point contact life equations [11] to [14] requires b^* and a^* b^*. For most ball bearings, the ratio of major to minor contact ellipse (a/b) ranges from 4 to 6. In this range, these solutions may be reproduced in Figure A2 at an enlarged scale. Clearly, a linear approximation to the solutions is not unreasonable. In this range, the solutions are fitted to the following equation:

$$a^*b^* = 1.247 + 1.775[F(\rho) - 0.80] \qquad \text{[A3]}$$

and

$$b^* = 0.544 + 0.836[F(\rho) - 0.80], \qquad \text{[A4]}$$

Thus, in lieu of solving the elliptical integrals, the above approximation may be used while implementing the life equations.

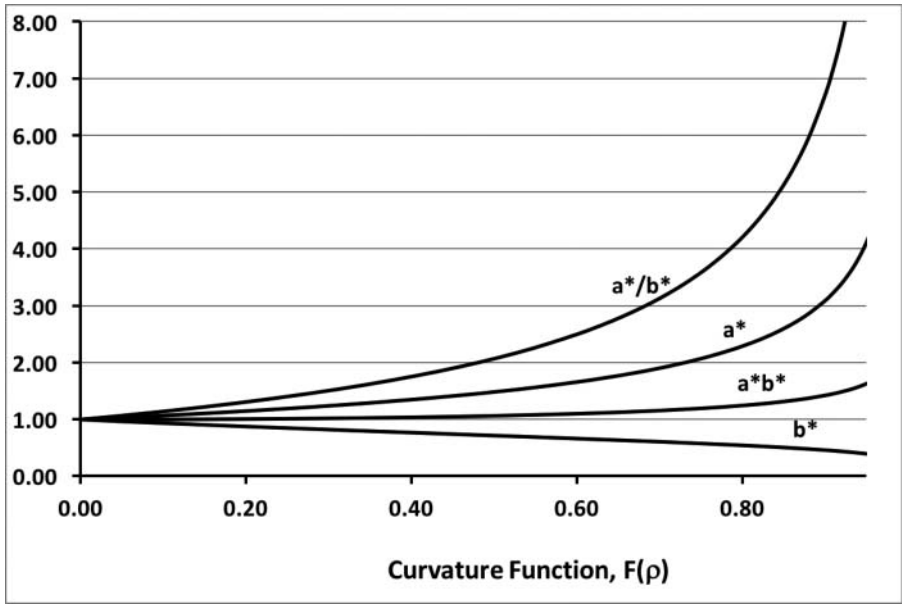

Figure A1. Elastic contact solution parameters as a function of curvature function.

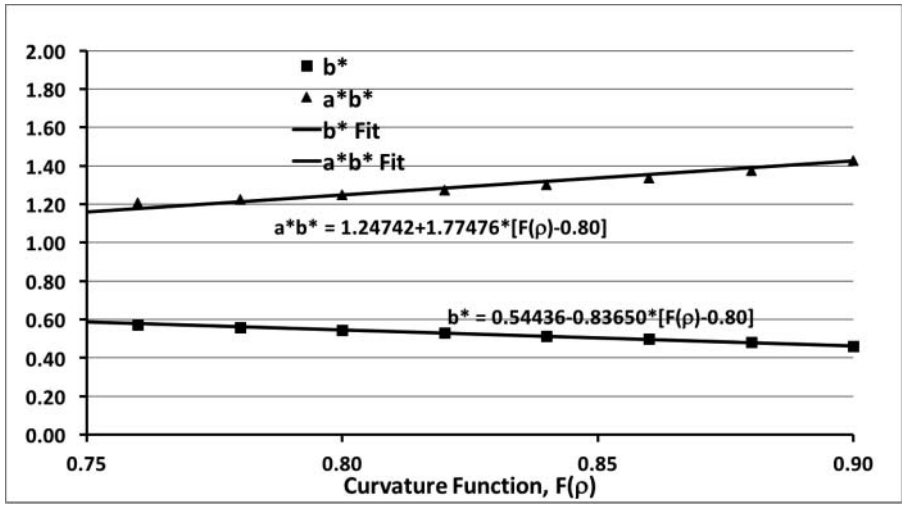

Figure A2. Elastic contact solution parameters in the range of geometry of most ball bearings.

Line contact elastic solutions

For a line contact configuration, as applicable to roller bearings, computation of the required contact parameters is simple in comparison to the point contact configuration. The contact parameters are simply defined as

$$a = \text{constant} \tag{A5a}$$

$$b = \left[\frac{2}{\pi a \sum \rho} \frac{Q}{E'}\right]^{1/2} \tag{A5b}$$

$$Q = \pi a b \bar{p}_H. \tag{A5c}$$

The major contact half width, a, is simply half of the roller to race contact length, and it is constant. The minor half-width is related to the applied load, bearing geometry, and material properties via Eq. [A5b], and Eq. [A5c] relates the contact load to contact pressure. Again, when developing the life equations in terms of pressure, the contact load may be eliminated in Eqs. [A5b] and [A5c] to express the contact half with in terms of pressure.

Shear stress–contact pressure relations

For any given rolling element–to-race contact, the applicable subsurface shear stress may also be related to Hertz contact pressure, p_H. Again, Harris and Kotzalas *(23)* have documented the ratios of both the maximum orthogonal shear stress, τ_o, and the maximum shear stress, τ_m, to the Hertzian contact pressure, p_H. Although the ratio of semiminor to semimajor axes of the contact ellipse, b/a, for point contact may vary arbitrarily, this ratio is less than 0.25 for most ball bearings; thus, it is quite reasonable to set this ratio to zero, as applicable to line contacts. Thus, the following line contact values of stress ratios

may be used in both point and line contact life equations [11] to [18]:

$$\frac{\tau_o}{p_H} = \zeta_{LP} = 0.25, \text{ and } \frac{z_o}{b} = \xi_{LP} = 0.50 \quad [A6]$$

and

$$\frac{\tau_m}{p_H} = \zeta_{GZ} = 0.30 \text{ and } \frac{z_m}{b} = \xi_{GZ} = 0.786. \quad [A7]$$

Stressed volume

The stressed volume is determined by contact width, w, normal to the rolling direction; depth of failure origination (z_o for the LP model and z_m for the GZ model); and the diameter of the track on the stressed element. Again, using a line contact approximation, the solutions for shear stress depth–to–contact half-width ratio, as documented by Harris and Kotzalas *(23)* may be used for both point and line contact equations:

$$\frac{z_o}{b} = \xi_{LP} = 0.50 \quad [A8]$$

and

$$\frac{z_m}{b} = \xi_{GZ} = 0.786. \quad [A9]$$

For contact width in roller bearings, with no misalignment, because the pressure along the roller length is uniform, the contact patch may be assumed as rectangular and the contact width may be set equal to roller length or twice the major half width ($w = 2a$). For ball bearings, however, because the pressure is elliptical along the contact length normal to the rolling direction, some assumption about effective contact width has to be made in order to compute the stressed volume. If the entire contact width is assumed to be stressed, then the contact width may be again set to twice the contact half-width and the contact patch may be assumed as rectangular. In order to preserve generality in the analysis, particularly for possible future modifications, the contact width is expressed as a fraction of contact half-width normal to the roller direction for both ball and roller bearings:

$$w = \eta a. \quad [A10]$$

The diameter of the track, d, on the races is equal to the race diameter at the contacting surface, and it will, of course, be different for outer and inner races. Though this diameter is equal to the diameter of race surface contacting the rollers in roller bearings, the applicable value of track diameter for angular-contact ball bearings is calculated from the bearing contact analysis under prescribed operating conditions. Thus, the stressed volume on the races for the LP and GZ models is expressed as

$$V_o = \pi d w z_o = \pi \eta d a b \xi_{LP} \quad [A11]$$

$$V_m = \pi d w z_m = \pi \eta d a b \xi_{GZ} \quad [A12]$$

for the LP and GZ models, respectively.

To compute the stressed volume in rolling elements, whereas the rollers in a roller bearing will just have one track along which the roller will contact the races, the balls in a ball bearing may precess and the total number of contact cycles may be distributed over multiple tracks. However, because the volume of each individual track is the same, the total effect may be closely simulated with one track, as for roller bearings. Thus, if the rolling element diameter is D, the stressed volume for both ball and rollers may be defined as

$$V_o = \pi D w z_o = \pi \eta D a b \xi_{LP} \quad [A13]$$

$$V_m = \pi D w z_m = \pi \eta D a b \xi_{GZ}. \quad [A14]$$

In order to develop the generalized ball and roller bearing stress life equations [11] to [18], all of the above point and line contact solutions are substituted in the fundamental life equations [8] and [10] to express life in terms of contact pressure.

Appendix B— Equations for dynamic load capacities

In the event that a load-based life equation is desired, the stress capacity equations introduced in this investigation can be easily converted to dynamic load capacity equations. Thus, corresponding to Eqs. [11] and [12], the dynamic load capacity of the LP point contact may be written as

$$Q_{cLP} = \hat{A}_{LP} \kappa_{LP}^{-\frac{3}{c+2-h}} \lambda_E^{-\frac{2c-2+h}{c+2-h}} \hat{G}_{LP}^{-\frac{3}{c+2-h}} u^{-\frac{3m}{c+2-h}} \quad [B1]$$

with

$$\hat{A}_{LP} = \frac{2}{3}\left[\frac{\pi^{3(c-1)}}{K_{LP}^3 E_o'^{2c+h-2}}\right]^{\frac{1}{c+2-h}} = \frac{2}{3}\,\pi^3 \frac{A_{LP}^3}{E_o'^2} \quad [B2a]$$

$$\hat{G}_{LPi} = d_i\left(\sum \rho\right)^{\frac{2c+h-2}{3}} a^{*1-c} b^{*1-c-h} \text{ for the races} \quad [B2b]$$

$$\hat{G}_{LPb} = D\left(\sum \rho\right)^{\frac{2c+h-2}{3}} a^{*1-c} b^{*1-c-h} \text{ for rolling elements} \quad [B2c]$$

$$\frac{1}{L_{LP}} = \left(\frac{Q}{Q_{cLP}}\right)^{\frac{c+2-h}{3m}}. \quad [B3]$$

Of course, both the stress capacity equations [11] and [12] and the above load capacity formulations provide identical lives.

For the GZ point contact equation, the dynamic load capacity, corresponding to the stress capacity in Eqs. [13] and [14], may be written as

$$Q_{cGZ} = \hat{A}_{GZ} \kappa_{GZ}^{-\frac{3}{cm+2}} \lambda_E^{-\frac{2(cm-1)}{cm+2}} \hat{G}_{GZ}^{-\frac{3}{cm+2}} u^{-\frac{3m}{cm+2}} \quad [B4]$$

with

$$\hat{A}_{GZ} = \frac{2}{3}\left[\frac{\pi^{3(cm-1)}}{{E'_o}^{2(cm-1)}K_{GZ}^3}\right]^{\frac{1}{cm+2}} = \frac{2}{3}\frac{\pi^3}{{E'_o}^2}A_{GZ}^3 \quad [B5a]$$

$$\hat{G}_{GZi} = d_i(a^*b^*)^{1-cm}\left(\sum\rho\right)^{\frac{2(cm-1)}{3}} \text{ for the races} \quad [B5b]$$

$$\hat{G}_{GZb} = D(a^*b^*)^{1-cm}\left(\sum\rho\right)^{\frac{2(cm-1)}{3}} \text{ for rolling elements} \quad [B5c]$$

$$\frac{1}{L_{GZ}} = \left(\frac{Q}{Q_{cGZ}}\right)^{\frac{cm+2}{3m}}. \quad [B6]$$

Similarly, for line contacts, the LP load capacity equation, corresponding to the stress capacity equations [15] and [16], may be defined as

$$\overline{Q}_{cLP} = \hat{B}_{LP}\kappa_{LP}^{-\frac{2}{c-h+1}}\lambda_E^{-\frac{c+h-1}{c-h+1}}\bar{\bar{G}}_{LP}^{-\frac{2}{c-h+1}}u^{-\frac{2m}{c-h+1}} \quad [B7]$$

with

$$\hat{B}_{LP} = \left(\frac{2^{c+h-1}\pi^{c-h-1}}{{E'_o}^{c+h-1}K_{LP}^2}\right)^{\frac{1}{c-h+1}} = \frac{2\pi}{E'_o}B_{LP}^2 \quad [B8a]$$

$$\bar{\hat{G}}_{LPi} = d_i a^{\frac{1+h-c}{2}}\left(\sum\rho\right)^{-\frac{1-h-c}{2}} \text{ for the races, and} \quad [B8b]$$

$$\bar{\hat{G}}_{LPb} = Da^{\frac{1+h-c}{2}}\left(\sum\rho\right)^{-\frac{1-h-c}{2}} \text{ for the rolling elements} \quad [B8c]$$

and

$$\frac{1}{L_{LP}} = \left(\frac{Q}{\overline{Q}_{cLP}}\right)^{\frac{c-h+1}{2m}}. \quad [B9]$$

For the GZ line contact models, Eqs. [17] and [18] may be converted to

$$\overline{Q}_{cGZ} = \hat{B}_{GZ}\kappa_{GZ}^{-\frac{2}{cm+1}}\lambda_E^{\frac{1-cm}{1+cm}}\bar{\bar{G}}_{GZ}^{-\frac{2}{cm+1}}u^{-\frac{2m}{cm+1}} \quad [B10]$$

with

$$\hat{B}_{GZ} = \left[\frac{(2\pi)^{cm-1}}{{E'_o}^{cm-1}K_{GZ}^2}\right]^{\frac{1}{cm+1}} = \frac{2\pi}{E'_o}B_{GZ}^2 \quad [B11a]$$

$$\bar{\bar{G}}_{GZi} = d_i\left(\frac{a}{\sum\rho}\right)^{\frac{1-cm}{2}} \text{ for the races, and} \quad [B11b]$$

$$\bar{\bar{G}}_{GZb} = D\left(\frac{a}{\sum\rho}\right)^{\frac{1-cm}{2}} \text{ for the rolling elements} \quad [B11c]$$

and

$$\frac{1}{L_{GZ}} = \left(\frac{Q}{\overline{Q}_{cGZ}}\right)^{\frac{cm+1}{2m}}. \quad [B12]$$

Discussion

Nikhil Londhe

Department of Mechanical & Aerospace Engineering, University of Florida, Gainesville, FL, USA.

In this work, the authors have certainly simplified life prediction methodology for rolling element bearings. Equations [11a]–[11k] are particularly useful. In addition, the capability to calculate separate lives for steel races and ceramic rolling elements is helpful. Due to the stress life model, the influence of operating temperatures can also be analyzed in detail. However, I wish to express the following concerns about the work presented in this article.

On the issue of fatigue limits for AISI 52100 bearing steel

The Hertzian stresses under which rolling contact fatigue (RCF) tests were conducted on SUJ2 material by Shimizu *(16)* are in the range of 4.3–5.2 GPa. These are very high compared to normal operating conditions of the majority of industrial bearings. Any RCF test at these loads will exhibit failure of rotating components. The Von Mises equivalent fatigue limit for carbon vacuum-degassed AISI 52100 steel is 684 MPa only (as per Harris and Barnsby *(29)*). Moreover, as per data given in Shimizu *(16)*, the fatigue test results at 0.22 GPa maximum shear stress, for which one of the two components was reported to have failed, is from alternating torsion fatigue tests. The authors should provide valid reasons for extending this structural fatigue observation to rolling contact fatigue, particularly given the fact that the two processes are fundamentally are very different. As per Shimizu *(16)*, the stress life exponent for RCF and alternating torsion fatigue were found to be similar; hence, it was reasoned that both fatigue behaviors are similar. This conclusion is derived only based on mathematical work. Though the underlying mathematics appear to be the same, the mechanics and material science involved in the two processes are completely different. Torsion fatigue is surface initiated, whereas RCF is subsurface initiated. Due to localized tri-axial loading, RCF involves phase transformation, microplasticity, and evolution of residual stress profiles in the subsurface region of the material. Various experimental investigations on 52100 bearing steel have confirmed these observations (Voskamp and Mittemeijer *(30)*; Voskamp, et al. *(31)*; Bhadeshia *(32)*; Bohmer, et al. *(33)*). In particular, due to phase transformations and microplasticity, the strength of the material is continuously evolving as a function of number of RCF cycles. This will influence the material's endurance performance under RCF loading. Comparison between rolling contact fatigue and alternating torsion fatigue can be made if similar metallurgical features/transformations are exhibited by the material under both types of loading. Can the authors provide any evidence if subsurface material transformations observed under RCF loading are also observed in alternating torsion fatigue tests as are reported in Shimizu *(16)* and Zaretsky *(17)*?

On the new fundamental GZ life equation

The Weibull slope captures the inherent variability in material microstructure. That is, it is guaranteed that the same amount of stress on nominally identical samples of material will produce different lives. Hence, the stress life exponent should include Weibull slope m. For example, the life of 52100 steel from manufacturer A will be different from that of manufacturer B under nominally identical loading conditions. This situation can be explained by having a stress life relation that is dependent on the Weibull slope parameter.

The assembly of terms in the new fundamental GZ life equation [10] comes with an inherent assumption that the entire volume V_m is subjected to maximum shear stress τ_m, which is incorrect. Based on Hertz theory, there exists a gradient in the stress field in the subsurface region. Only the point at a critical depth of z_m is subjected to maximum shear stress τ_m; the entire surrounding region experiences lower stresses. Setting aside the issue of fatigue limits, Ioannides and Harris's *(15)* model can be considered an improvement over the LP model because it accounted for this fact. The stress integral used in Ioannides and Harris's *(15)* model captures this gradient in stress field in the RCF-affected region.

In Eq. [11b], parameter Φ_{LP} is used to adjust the empirical life constant. Is this parameter the same as STLE life factors published in Zaretsky *(13)*? In addition, is it dependent on the material parameter λ_E defined in Eq. [11h]? Clarifications on this will enable effective use of the model presented in this work.

Equations [19] and [20] are derived based on the assumption that K_{LP} and K_{GZ} are the same for both point and line contacts, respectively. The authors should justify this assumption or provide experimental evidence to support the same. Even though K_{LP} and K_{GZ} are constants, they can take different values in Eqs. [7] and [10] for different test settings. They are applicable for specific test configurations and operating conditions.

In this analysis, the influence of temperature on elastic modulus is considered for the determination of L_{10} life. No consideration is given to the strength of the material, which will also decrease with increasing temperatures. For example, experimental data from Bohmer, et al. *(33)* show a decrease in endurance strength with increasing temperatures. These results contradict the plot shown in Fig. 7. Can the authors justify these experimental observations (from Bohmer, et al. *(33)*) with the stress life model proposed in this work?

In this work, the authors have provided a simplified stress life approach for bearing fatigue life calculation. It will certainly help researchers to compute bearing life with minimal efforts. However, determination of contact stresses remains a computationally challenging task for composite materials such as case-carburized bearing steels. Can the authors discuss how this proposed stress life method can be used for case-carburized bearing steels that have an inhomogeneous microstructure and linearly varying material properties in the subsurface region near the contact?

References

(29) Harris, T. A. and Barnsby, R. M. (2001), "Life Ratings for Ball and Roller Bearings," *Proceedings of the Institution of Mechanical Engineers - Part J: Journal of Engineering Tribology*, **215**(6), pp 577–595.

(30) Voskamp, A. P. and Mittemeijer, E. J. (1997), "State of Residual Stress Induced by Cyclic Rolling Contact Loading," *Materials Science and Technology*, **13**, pp 430–438.

(31) Voskamp, A. P., Osterlund, R., Becker, P. C., and Vingsbo, O. (1980), "Gradual Changes in Residual Stress and Microstructure during Contact Fatigue in Ball Bearings," *Metal Technology*, **7**, pp 14–21.

(32) Bhadeshia, H. K. D. H. (2012), "Steels for Bearings," *Progress in Materials Science*, **57**(2), pp 268–435.

(33) Bohmer, H. J., Losche, T., Ebert, F. J., and Streit, E. (1999), "The Influence of Heat Generation in the Contact Zone on Bearing Fatigue Behavior," *Journal of Tribology*, **121**, pp 462–467.

Authors' Response

The authors would like to thank Nikhil Londhe for his thoughtful comments and issues that he presents. Bhadeshia *(32)* has compiled and summarized 953 references pertaining to bearing steels. Following the work of Ioannides and Harris *(15)*, Harris and Barnsby *(29)* advocated the incorporation and application of a fatigue limiting stress for rolling element bearing fatigue life calculations. The increase in life at low stresses due to compressive residual stresses is often mistaken or confused with that obtained by applying a fatigue limiting stress, below which there is no fatigue. The present work, however, is not related to any fatigue-limiting stress for rolling element fatigue. The fatigue life models discussed by the authors are completely based on subsurface shear stresses.

At an ASTM symposium on rolling contact fatigue testing of bearing steels held from May 12 to 14, 1981, in Phoenix, Arizona, Lorosch *(34)*, of the FAG Bearing Company (now part of INA-Schaeffler KG) presented results of full-scale bearing fatigue tests on three groups of vacuum-degassed, 7205B-size AISI 52100 inner races at maximum Hertz stresses of 2.6, 2.8, and 3.5 GPa (370, 406, and 500 ksi), respectively. From these tests, Lorosch *(34)* concluded that "under low loads and with elastohydrodynamic lubrication, there is no material fatigue." However, at the same ASTM conference, Zwirlein and Schlicht *(35)*, also of the FAG Bearing Company, used the same 7205B-size bearing inner races and reported large amounts of compressive residual stresses due to the transformation of retained austenite into martensite. Pioneering bearing research performed at the General Motors Research Center in Warren, Michigan, through the 1960s (Almen *(36)*;Bush, et al. *(37)*; Koistinen *(38)*; Gentile, et al. *(39)*; Gentile and Martin *(40)*) showed that these compressive residual stresses can significantly increase bearing fatigue life.

To confirm the General Motors results, Parker and Zaretsky *(41)* made residual stress measurements on several 207-size, deep-groove ball bearings that were run for different times to determine a prestress cycle suitable for inducing significant compressive residual stresses in the inner race–ball groove; this work has also been later reproduced in Zaretsky *(12)*. Compressive residual stresses greater than 0.7 GPa (100 ksi) were induced in the maximum shear stress region of the bearing inner races, which were run for 25 h at a maximum Hertz stress of 3.3 GPa (480 ksi). The lives attained with these prestressed bearings were compared with baseline fatigue tests carried out with bearings without a prestress cycle, run under

identical test conditions at a maximum Hertz stress of 2.4 GPa (350 ksi). The L_{10} life of the prestressed ball bearings was greater than twice that of the baseline bearings. Additionally, after 3,000 to 4,000 h of testing, the difference between the measured residual stresses in the prestressed and baseline bearings was small; in other words, both sets of bearings had high and equal levels of compressive residual stresses. Thus, the notable increase in life reported by Lorosch *(34)* may very well be explained by the presence of induced compressive residual stresses in the bearing raceways.

Although the parametric studies in the current article do not include life modeling as a function of residual stresses, implementation of these stresses in the newly developed stress-based life equations is quite straightforward in comparison to the widely used load-based equations.

Based on the above works, it can reasonably be concluded that the material phase transformations are a function of time, temperature, and stress, as well as the amount of retained austenite in the steel structure, as indicated by the studies of Voskamp and Mittemeijer *(30)* and Voskamp, et al. *(31)*. However, these subsurface phase transformations are not a condition precedent to fatigue crack initiation as implied by Londhe. Accordingly, if the bearing steel has low amounts (less than 5%) of retained austenite, we would not expect to observe subsurface material transformations, such as that described by Voskamp and Mittemeijer *(30)* and Voskamp, et al. *(31)*, in either rolling contact or alternating torsion fatigue tests, such as those reported by Shimizu *(16)* and Zaretsky *(17)*. The work of Shimizu *(16)* is simply used to demonstrate that the reported shear stress life exponent $c = 10.34$ is very much in line with the one proposed in this article, $c = 10.33$, in the newly introduced GZ life equation.

With regard to the validity of shear stress exponent obtained from torsion tests to rolling contact, it should be noted that the shear stress-life exponent only defines variation of life with applicable shear stress and not the total life. In other words, the shear stress-life exponent will remain unchanged as a function of residual stresses. From a mechanics standpoint, at any prescribed shear stress, if failures are related to this shear stress, then only the magnitude of shear stress is important; the process of how it is generated, torsion or rolling contact fatigue, is irrelevant.

In response to the question about applicability of tests conducted by Shimizu *(16)* in the maximum Hertz stress range of 4.3 to 5.2 GPa (657 to 754 ksi) to normal operating Hertzian stress levels for industrial bearings, which are usually under 2 GPa (300 ksi), the research conducted and summarized by Zaretsky, et al. *(42)* established, with reasonable engineering and statistical certainty, a qualitative correlation between rolling element fatigue tests in the NASA five-ball fatigue tester at maximum Hertz stress of 5.52 GPa (800 ksi) and those in full-scale bearing run at maximum Hertz stresses equal to or less than 2.4 GPa (350 ksi). Vlcek and Zaretsky *(43)* further document the correlation of bench-type tests with full-scale bearing results.

The effect of microstructural variation in the material matrices on life are generally associated with the volume of the material stressed. To account for such variations, the volume exponent in both the LP and GZ life equations includes data variability defined by the Weibull slope. As explained in the article, in the new GZ equation, only the shear stress exponent is independent of data variability. In addition, the GZ equation only eliminates the explicit variation in depth of the critical shear stress leading to failure. The implicit variation in depth still remains part of the stressed volume. In fact, because the depth of maximum shear stress in the GZ model is somewhat larger than that corresponding to the maximum orthogonal shear stress in the LP model, the stressed volume in the GZ model is larger in comparison to that in the LP model. Thus, the GZ life equation does permit variation in the microstructure of materials.

Due to the statistical nature of rolling element bearing life, all life models include an empirical constant, which is determined by correlating model predictions with experimentally measured lives with reasonable certainty. Therefore, the simple expression for stressed volume, in both the LP and GZ equations, is no more than symbolic and, as explained in the article, the effect of contact stress gradients and the resulting variation in stressed volume is included in the empirical constant.

With regard to the introduction of adjustment factor, Φ, in both the LP and GZ equations, it should be emphasized that this adjustment factor is only for future use to provide any adjustment to the base life constants for factors not considered in the models presented; presently, in both the LP and GZ models, it is simply set to 1.0. The factor Φ neither represents the commonly used "life adjustment factors" (Zaretsky *(13)*) nor has any specific relationship to the elastic properties of the material.

Because the base fatigue hypotheses presented in Eqs. [7] and [8] only relate life to subsurface shear stress and volume of material stressed, only the magnitude of these variables is significant. Practical applications, such as point or line contacts, in which these quantities are generated remain irrelevant from a mechanics standpoint. The empirical proportionality constants K_{LP} and K_{GZ} are, therefore, applicable to both point and line contact configurations. The effect of a specific type of contact is, of course, included in the actual computation of shear stress and the stressed volume, as explained in the article. It must be emphasized that the constants K_{LP} and K_{GZ}, respectively, in the LP and GZ models are base model constants. They are similar to the constants A and B, commonly used in point and line contact life equations. These constants do not depend on bearing operating conditions. In fact, as discussed in the article, the constants A and B are actually related via the base respective constant K. Furthermore, the LP and GZ models, due to different shear stress exponents and due to the absence of the shear stress depth term in the GZ model, are distinctly different.

In the parametric examples showing the effect of operating temperature on life, the authors would like to repeat their comment that the present investigation only considers the effect of variation in elastic modulus as a function of temperature. The elastic properties completely define the applicable shear stresses, which essentially constitute the base life models.

The role of change in endurance strength with change in temperature, as discussed by Bohmer, et al. *(33)*, is a subject for future investigations. It is also well understood that increasing

operating temperature reduces the functional hardness of the bearing steel, which in turn reduces fatigue life. The effect of hardness on life is generally applied as a life adjustment factor on the computed basic life, as discussed by Zaretsky *(12), (13)*. Perhaps other life adjustment factors, such as those due to change in material behavior pointed out by Bohmer, et al. *(33)*, may be developed in the future.

Indeed, the computations of contact and subsurface stresses are generally restricted to homogeneous elastic materials. For nonhomogeneous materials, such as case-carburized steel, in which the elastic properties may vary with depth, both contact and subsurface stress modeling are challenging. Even if sophisticated finite element or finite difference models are developed for such problems, implementation of these models in an actual bearing with multiple contacts may be computationally impractical. A more practical approach may be to compute an "effective" elastic modulus by carrying out applicable analyses for specific contact configurations of interest.

References

(34) Lorosch, H. K. (1982), "Influence of Load on the Magnitude of the Life Exponent for Rolling Bearings," *Rolling Contact Fatigue Testing of Bearing Steels*, Hoo, J. J. C. (Ed.), ASTM STP-771, pp 275–292, American Society for Testing and Materials: Philadelphia, PA.

(35) Zwirlein, O. and Schlicht, H. (1982), "Rolling Contact Fatigue Mechanisms—Accelerated Testing Verses Field Performance," *Rolling Contact Fatigue Testing of Bearing Steels*, Hoo, J. J. C. (Ed.), ASTM STP-771, pp 358–379, American Society for Testing and Materials: Philadelphia, PA;

(36) Almen, J. O. (1962), "Effects of Residual Stress on Rolling Bodies," *Rolling Contact Phenomena*, Bidwell, J. B. (Ed.), pp 400–424, Elsevier Publishing Company: New York.

(37) Bush, J. J., Grube, G. H., and Robinson, G. H. (1962), "Microstructural and Residual Stress Changes in Hardened Steel due to Rolling Contact," *Rolling Contact Phenomena*, Bidwell, J. B. (Ed.), pp 365–399, Elsevier Publishing Company: New York.

(38) Koistinen, D. P. (1964), "The Generation of Residual Compressive Stresses in the Surface Layers of Through-Hardened Steel Components by Heat Treatment," *ASM Transactions*, **57**, pp 581–588.

(39) Gentile, A. J., Jordan, E. F., and Martin, A. D. (1965), "Phase Transformations in High-Carbon, High-Hardness Steels under Contact Loads," *AIME Transactions*, **233**(6), pp 1085–1093.

(40) Gentile, A. J. and Martin, A. D. (1965), "The Effect of Prior Metallurgically Induced Compressive Residual Stress on the Metallurgical and Endurance Properties of Overload Tested Ball Bearings," **ASME Paper 65-WA/CF-7**.

(41) Parker, R. J. and Zaretsky, E. V. (1972), "Effect of Residual Stresses Induced by Prestressing on Rolling-Element Fatigue Life," **NASA TN D-6995**.

(42) Zaretsky, E. V., Parker, R. J., and Anderson, W. J. (1982), "NASA Five-Ball Fatigue Tester—Over 20 Years of Research," *Rolling Contact Fatigue Testing of Bearing Steels*, Hoo, J. J. C. (Ed.), ASTM STP-771, pp 5–45, American Society for Testing and Materials: Philadelphia, PA.

(43) Vlcek, B. L. and Zaretsky, E. V. (2011), "Rolling-Element Fatigue Testing and Data Analysis—A Tutorial," *Tribology Transactions*, **54**(4), pp 523–541.